



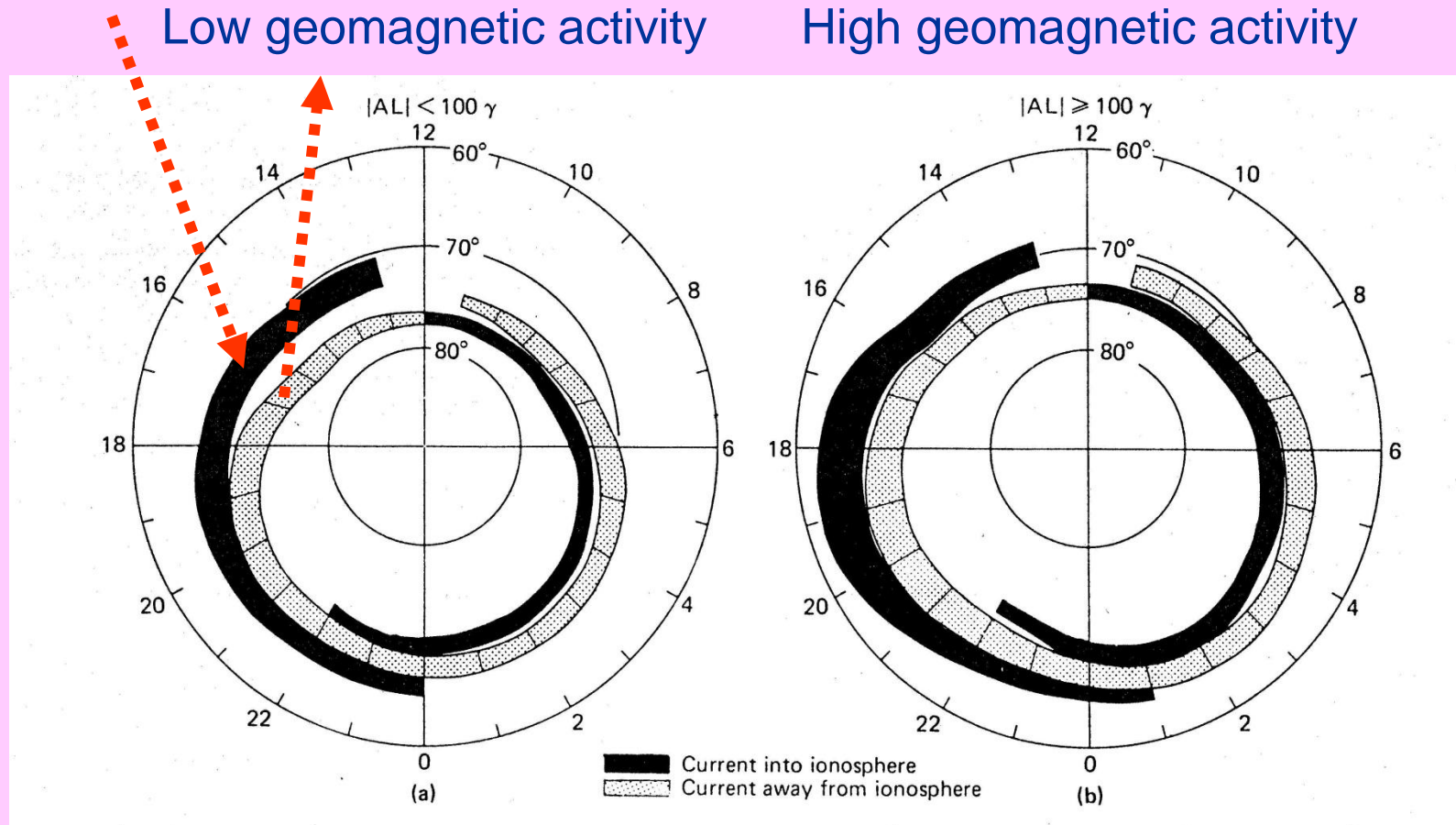
Last lecture (8)

- Magnetospheric dynamics
- Geomagnetic activity
- Cosmic radiation

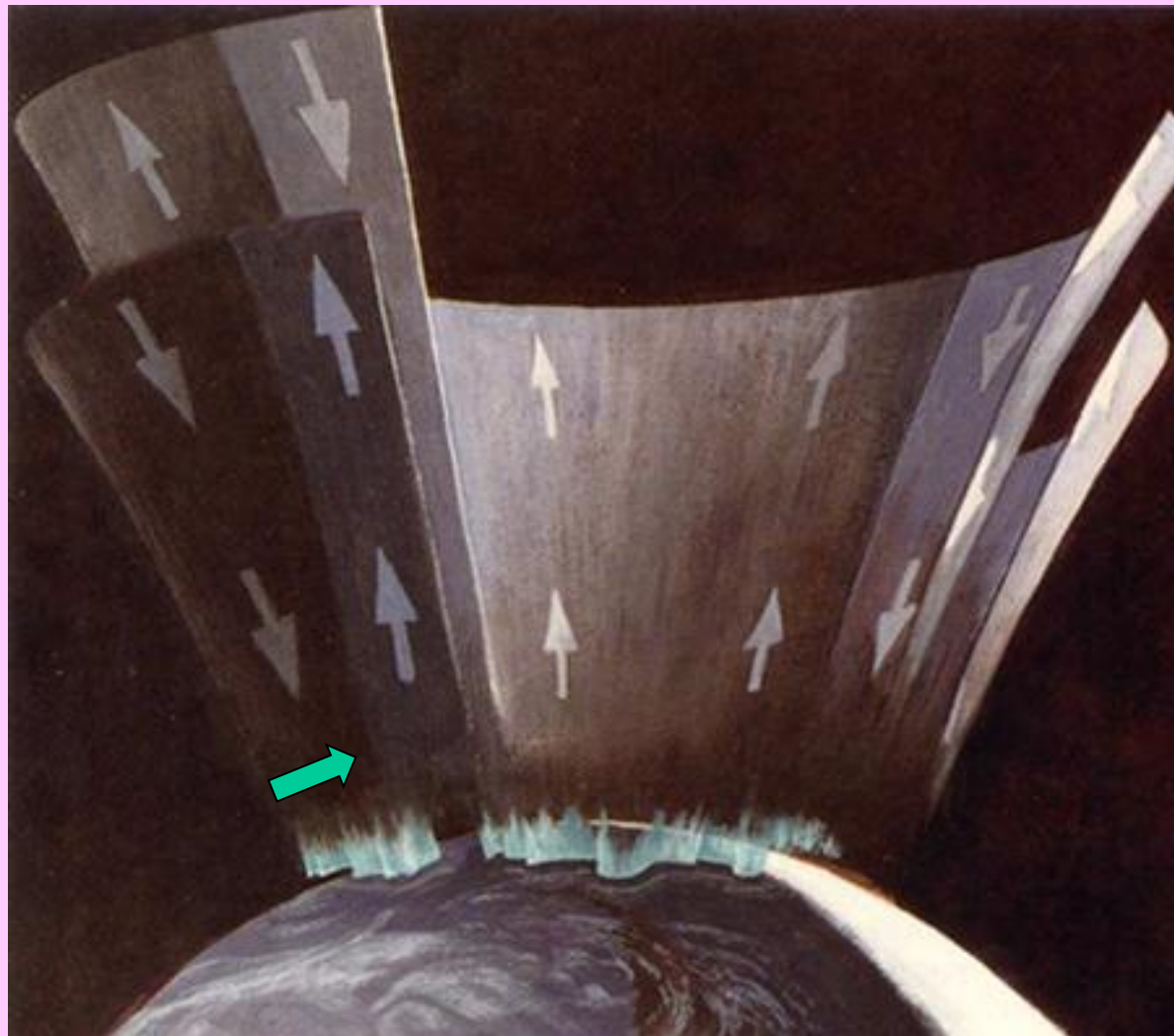
Today's lecture (9)

- Interstellar plasma
- Alfvén waves

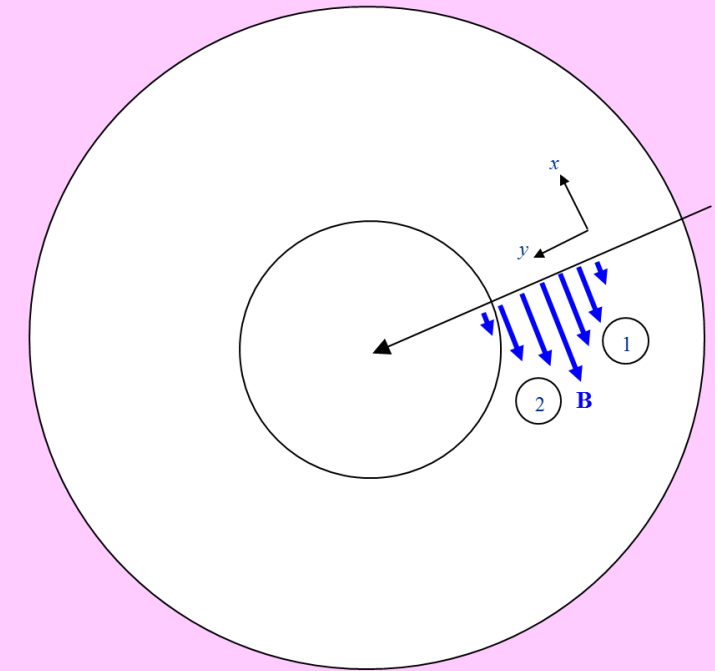
Birkeland currents in the auroral oval



Birkeland currents in the auroral oval



Mini-groupwork 5



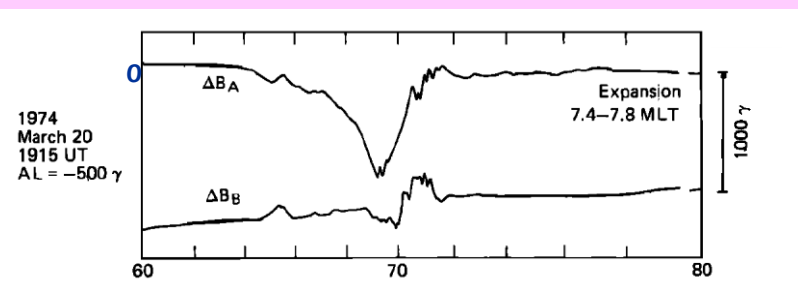
Current sheet 1: $j_z = -\frac{1}{\mu_0} \frac{\partial B_x}{\partial y}$

$$\frac{\partial B_x}{\partial y} < 0 \quad \Rightarrow \quad j_z > 0$$

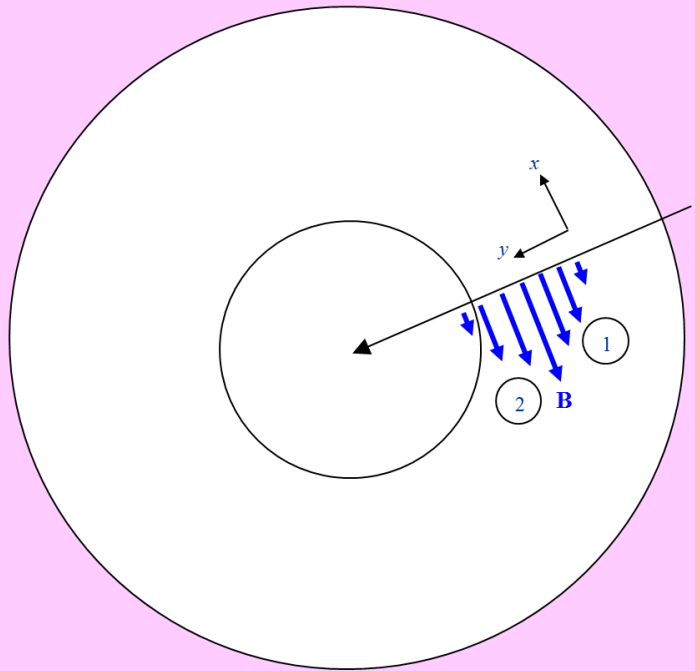
$$\Delta B_x \approx -\frac{15 \text{ mm}}{22 \text{ mm}} \cdot 1000 \cdot 10^{-9} = -6.8 \cdot 10^{-7} \text{ T}$$

$$\Delta y \approx \frac{10 \text{ mm}}{10 \text{ mm}} \cdot \frac{2^\circ}{360^\circ} 2\pi (R_E + 800 \text{ km}) = 250 \cdot 10^3 \text{ m}$$

$$j_z \approx -\frac{1}{\mu_0} \frac{\Delta B_x}{\Delta y} = 2.2 \cdot 10^{-6} \text{ Am}^{-2}$$



Mini-groupwork 5



Current sheet 2:

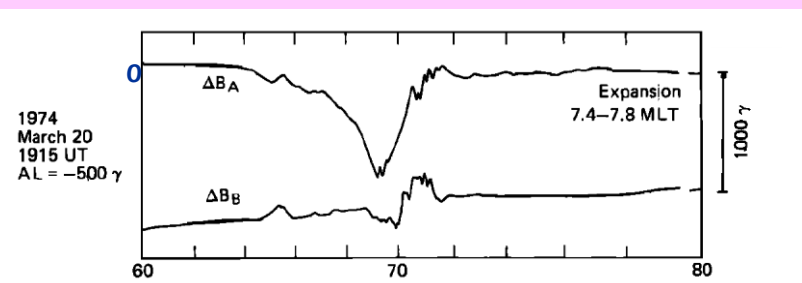
$$j_z = -\frac{1}{\mu_0} \frac{\partial B_x}{\partial y}$$

$$\frac{\partial B_x}{\partial y} > 0 \quad \Rightarrow \quad j_z < 0$$

$$\Delta B_x \approx \frac{18 \text{ mm}}{22 \text{ mm}} \cdot 1000 \cdot 10^{-9} = 6.8 \cdot 10^{-7} \text{ T}$$

$$\Delta y \approx \frac{10 \text{ mm}}{10 \text{ mm}} \cdot \frac{2^\circ}{360^\circ} 2\pi (R_E + 800 \text{ km}) = 250 \cdot 10^3 \text{ m}$$

$$j_z \approx -\frac{1}{\mu_0} \frac{\Delta B_x}{\Delta y} = -2.6 \cdot 10^{-6} \text{ Am}^{-2}$$

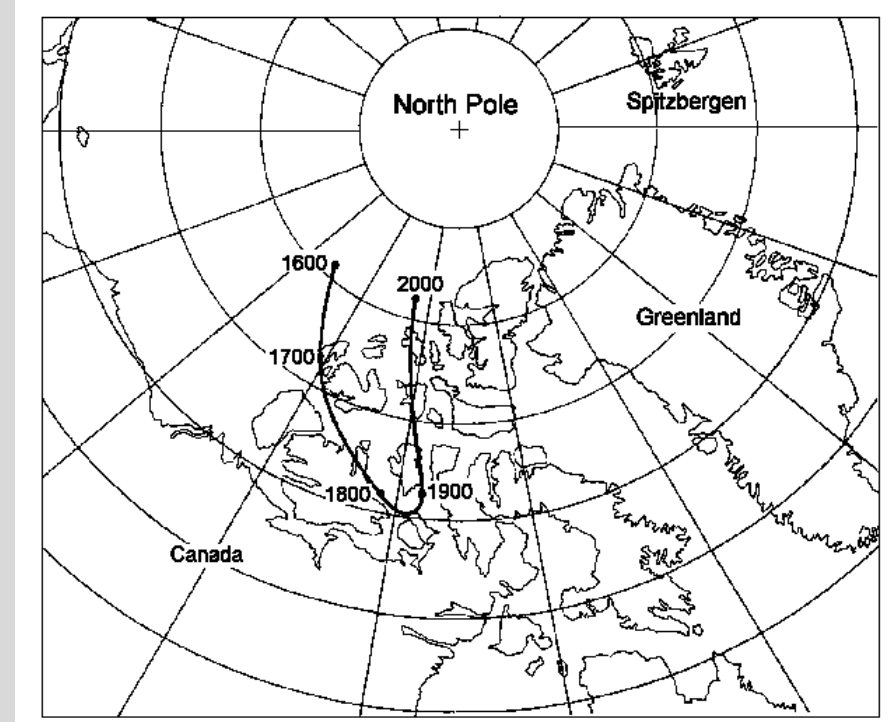
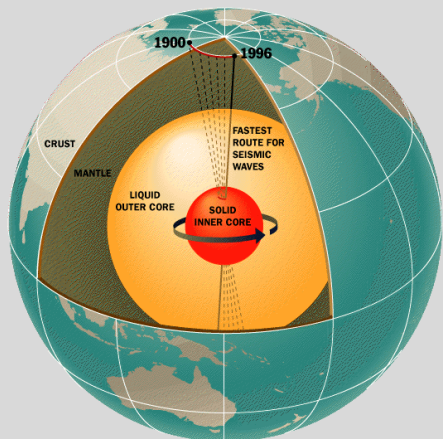
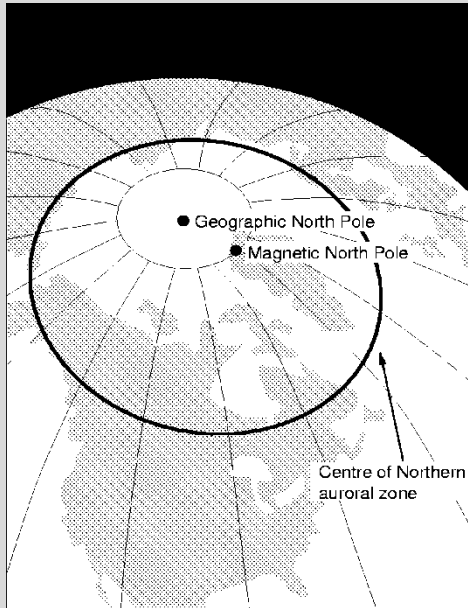




Questions

- 1. Changes between open and closed all the time?**
- 2. Secondary cosmic rays are made in atmosphere?**
- 3. Cosmic rays present allt he time?**
- 4. Geomagnetic field changes?**
- 5. Why can't you see blue aroras?**

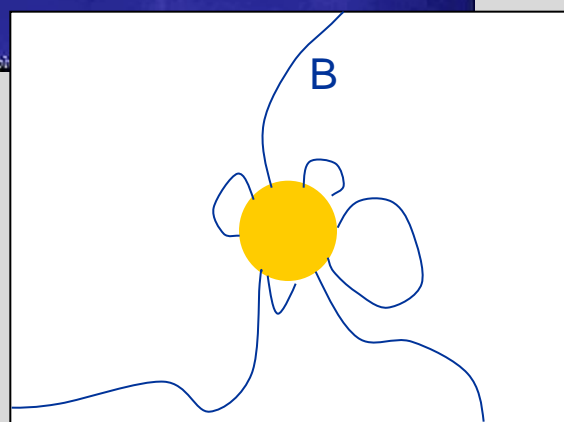
Motion of the magnetic pole



Different from geomagnetic reversals (time scale 1 million years). most recent such event, called the Brunhes-Matuyama reversal, occurred about 780,000 years ago.

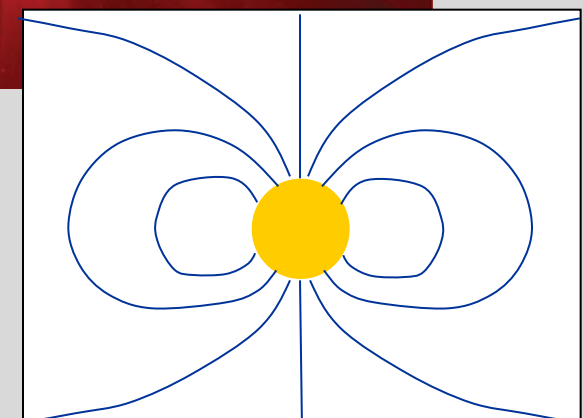
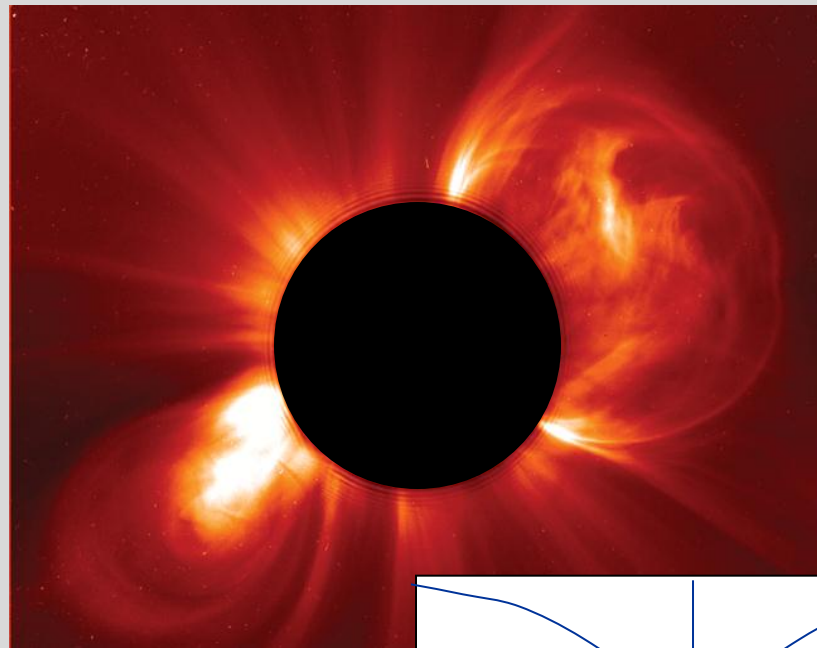
Solar magnetic field as organizing factor

Maximum



Maximum: weak, irregular magnetic field

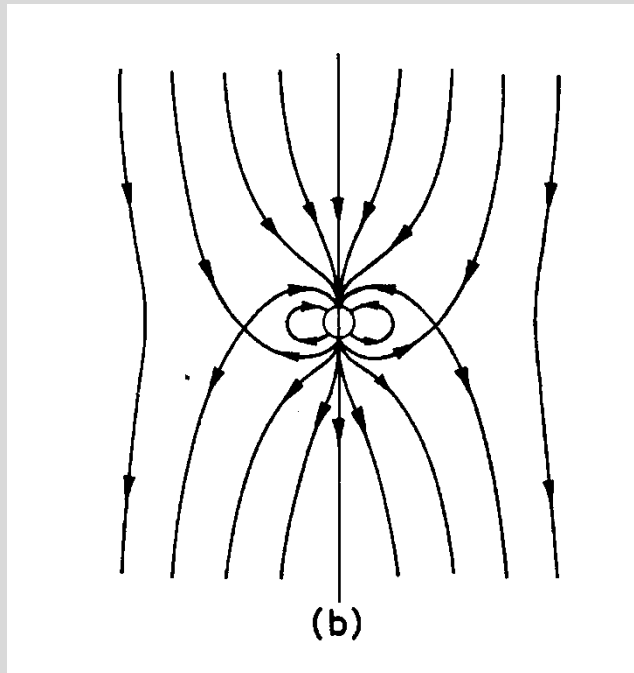
Minimum



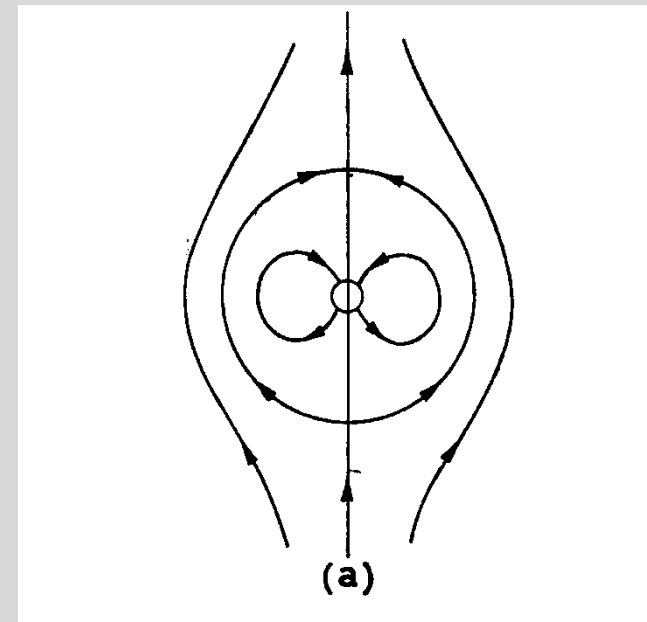
Minimum: large, regular dipole-like field

Magnetospheric dynamics

open magnetosphere



closed magnetosphere

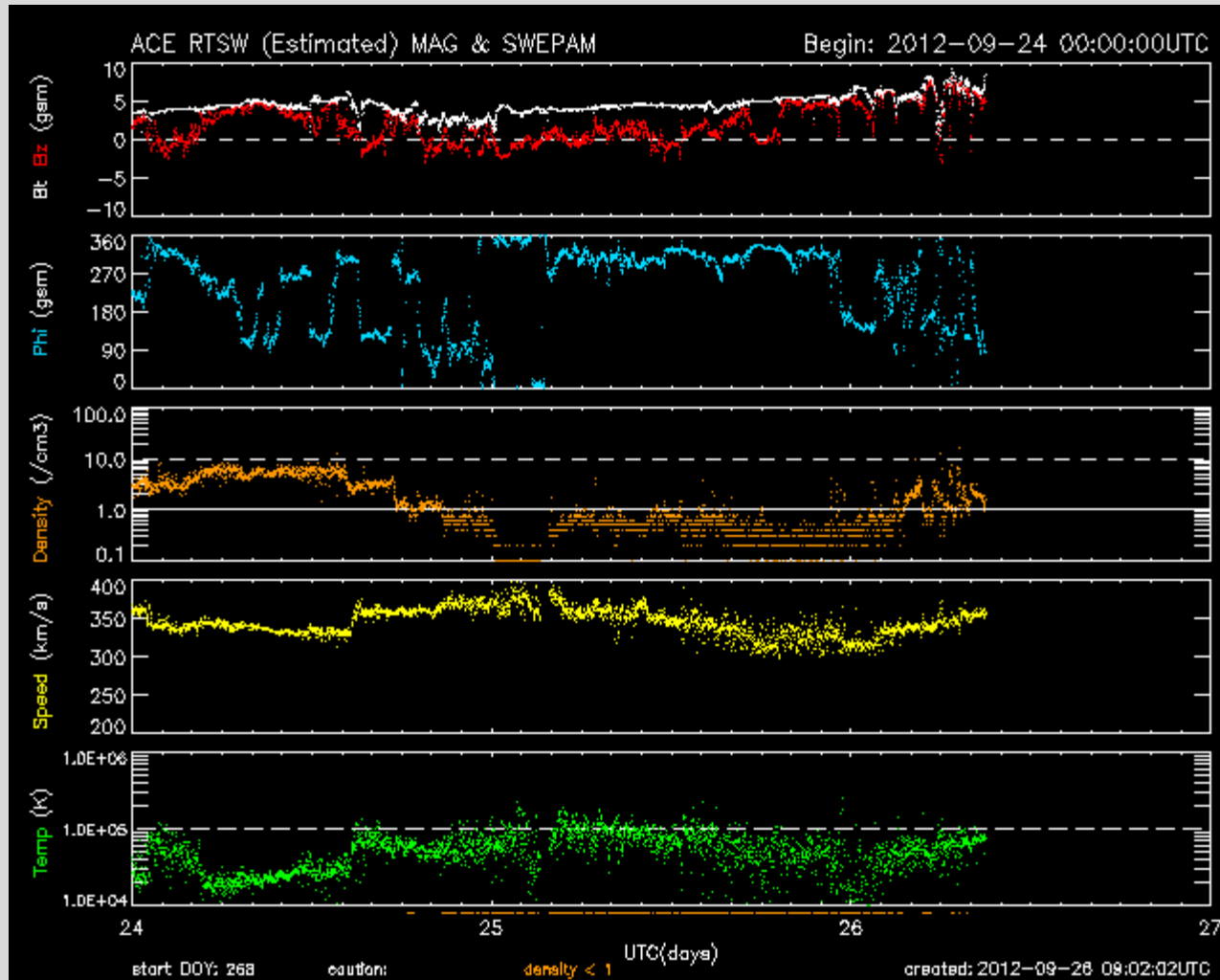


southward 

Interplanetary
magnetic field (IMF)

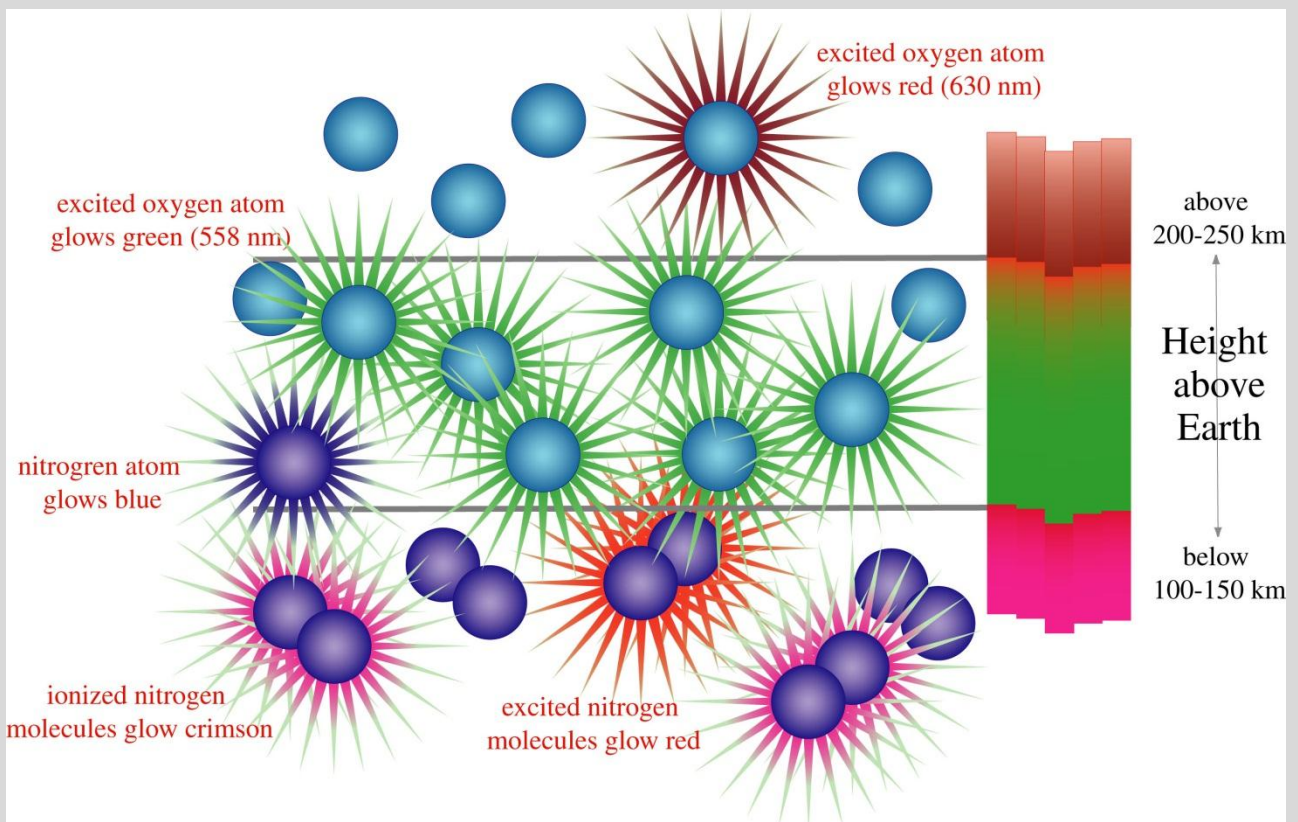
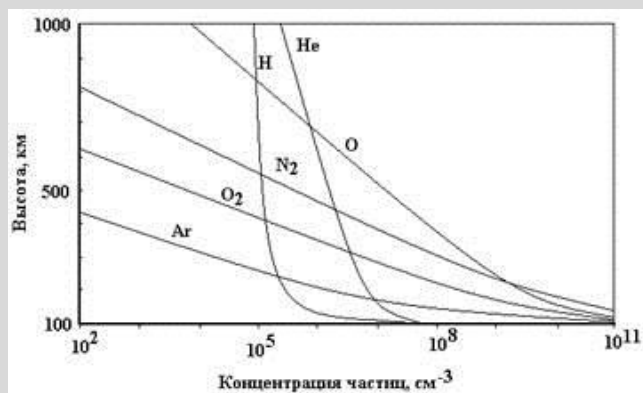
 northward

Solar wind magnetic field





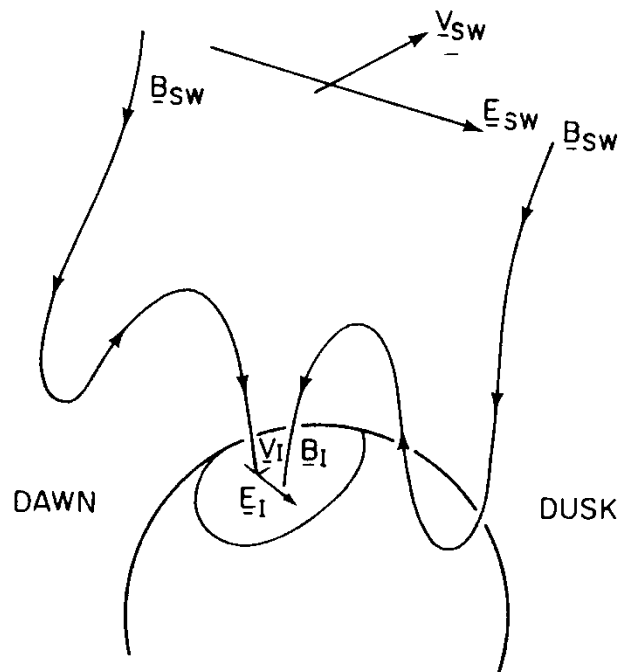
Emissions



Magnetospheric dynamics

open magnetosphere

Viewpoint 1



The solar wind generates an electric field

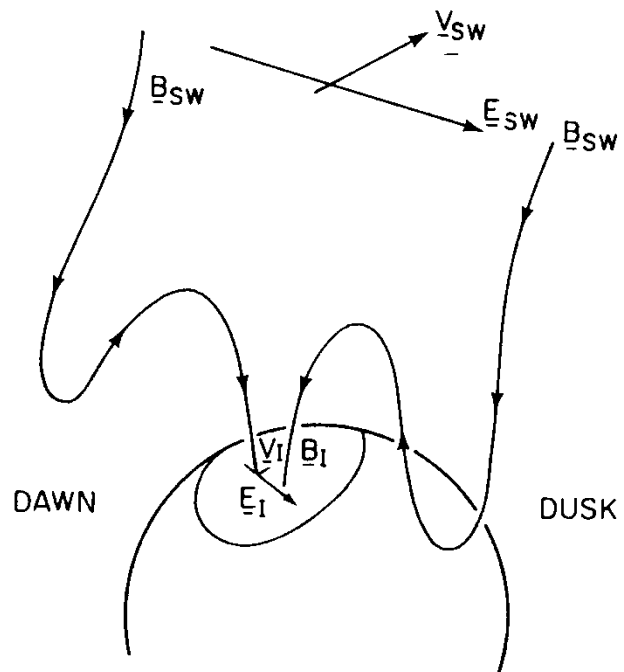
$$\mathbf{E}_{SW} = - \mathbf{v}_{SW} \times \mathbf{B}_{SW}$$

which maps down to the ionosphere, since the field lines are very good conductors

Magnetospheric dynamics

open magnetosphere

Viewpoint 2



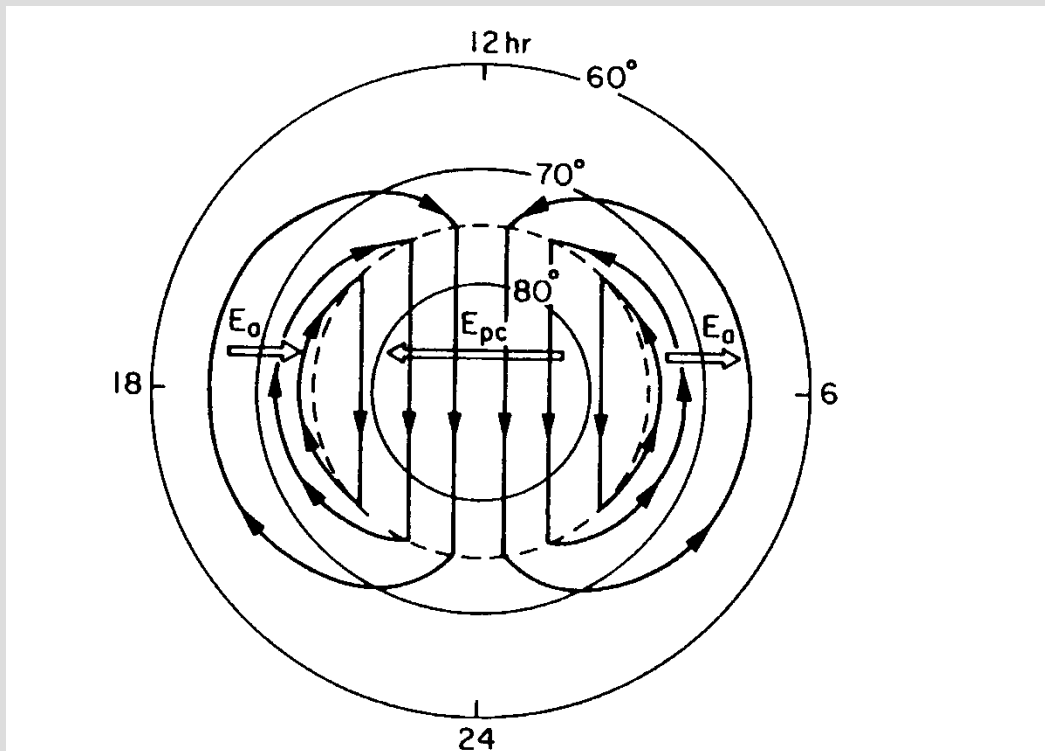
The solar wind magnetic field draws the ionospheric plasma with it, since the field is frozen into the plasma. This motion induces an ionospheric electric field

$$\mathbf{E}_I = - \mathbf{v}_I \times \mathbf{B}_I$$

Magnetospheric dynamics

The electric field "propagates" to the ionosphere, since the field lines are good conductors, and thus equipotentials

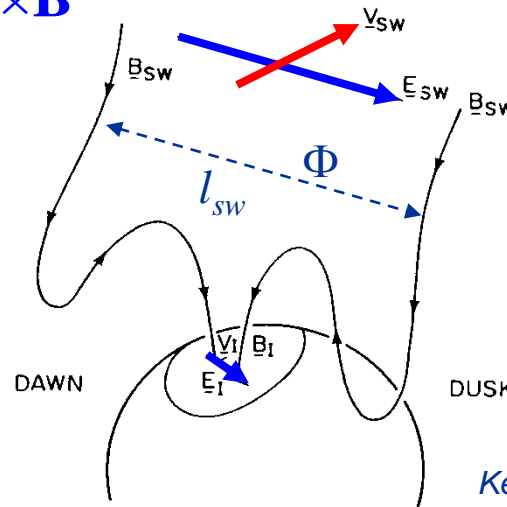
Plasma convection in the ionosphere



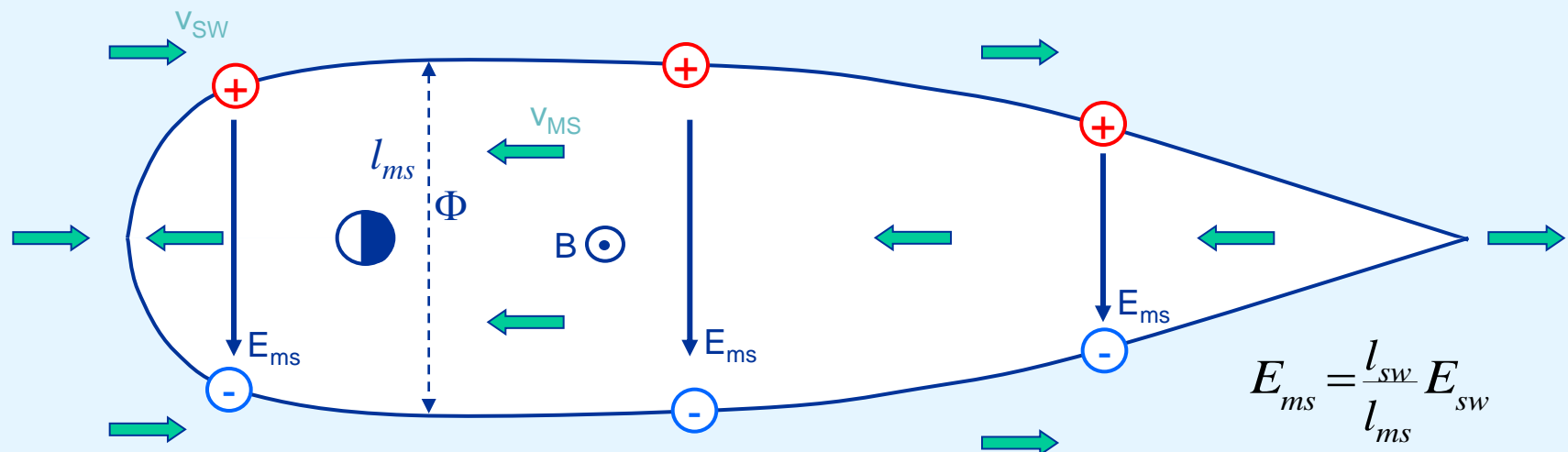
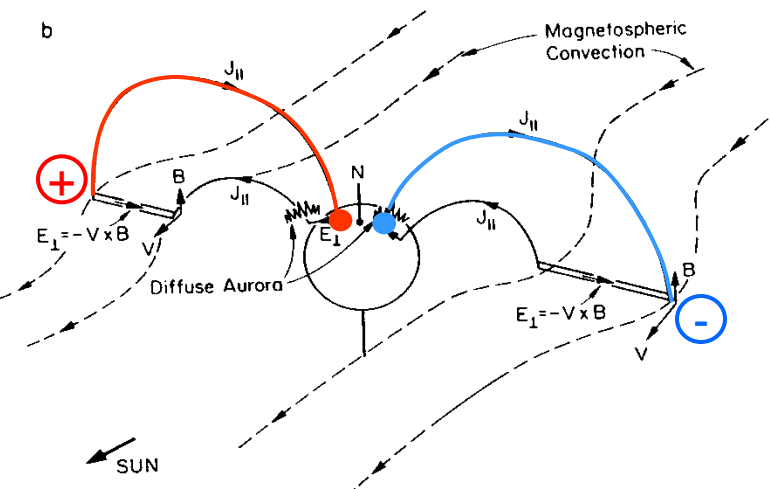
Magnetospheric plasma convection



$$\mathbf{E}_{sw} = -\mathbf{v} \times \mathbf{B}$$

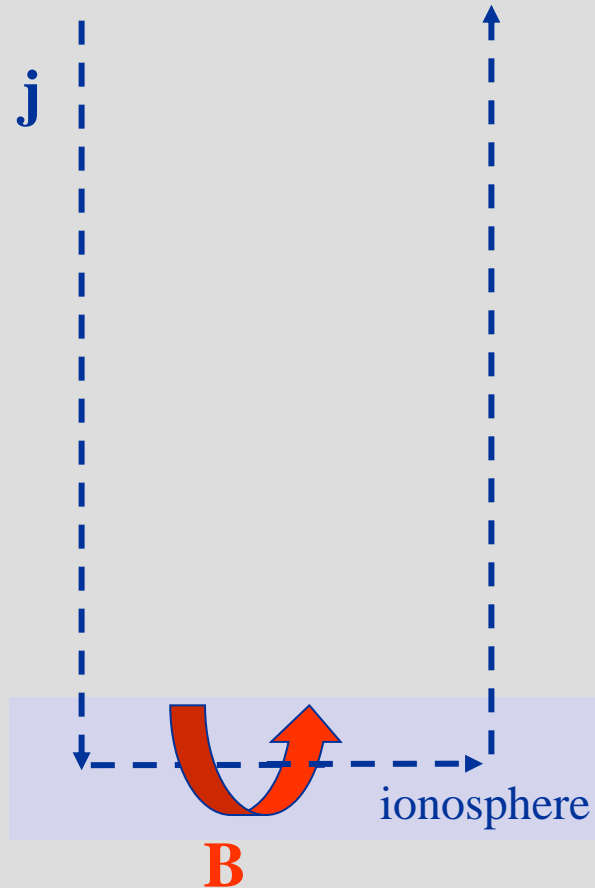


Kelley, 1989



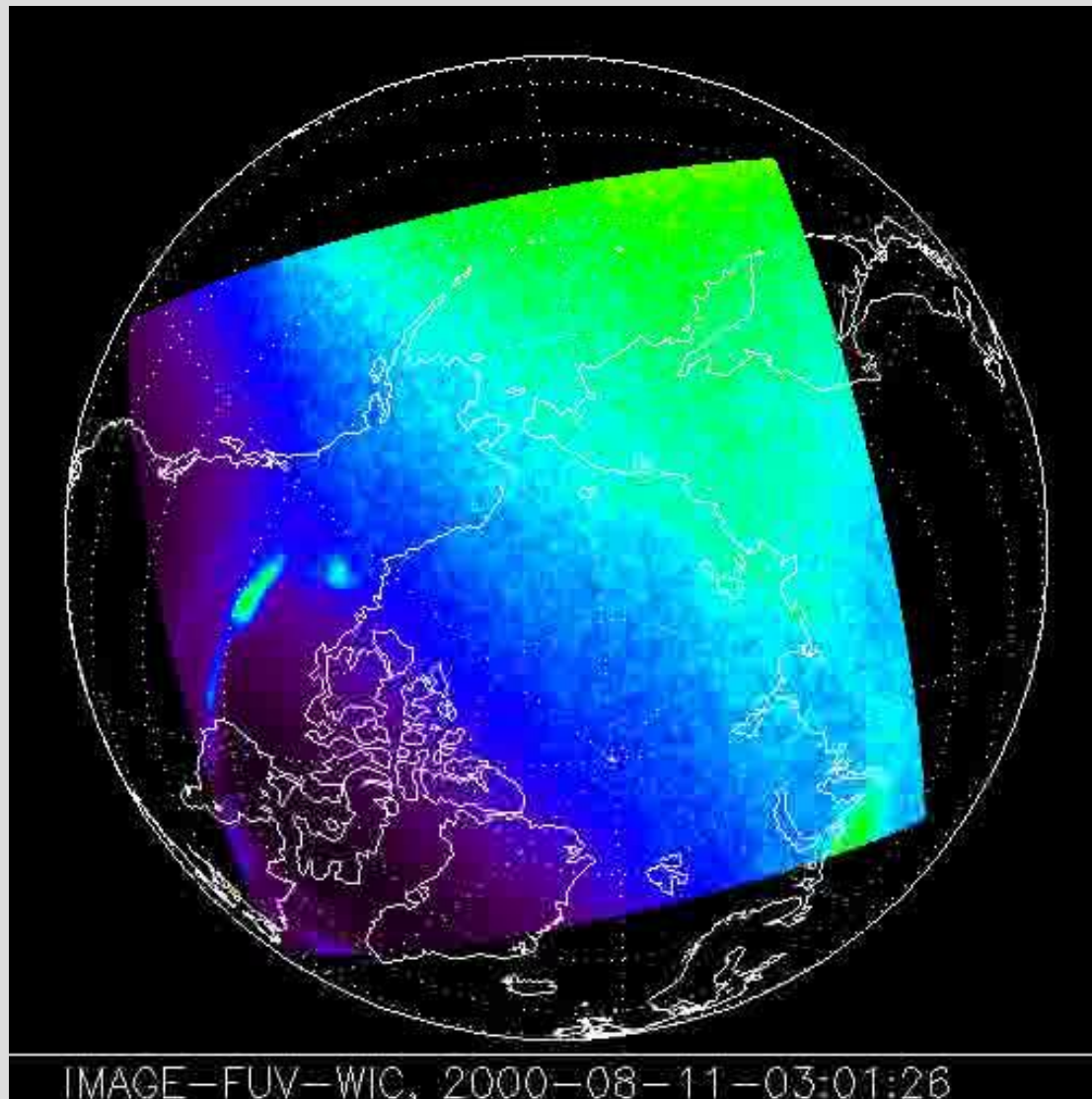
Geomagnetic activity, definition

- Geomagnetic activity = temporal variations in the geomagnetic field.
- These variations are caused by temporal variations in the currents in the magnetosphere and ionosphere.
- The variations are observed by geomagnetic observatories

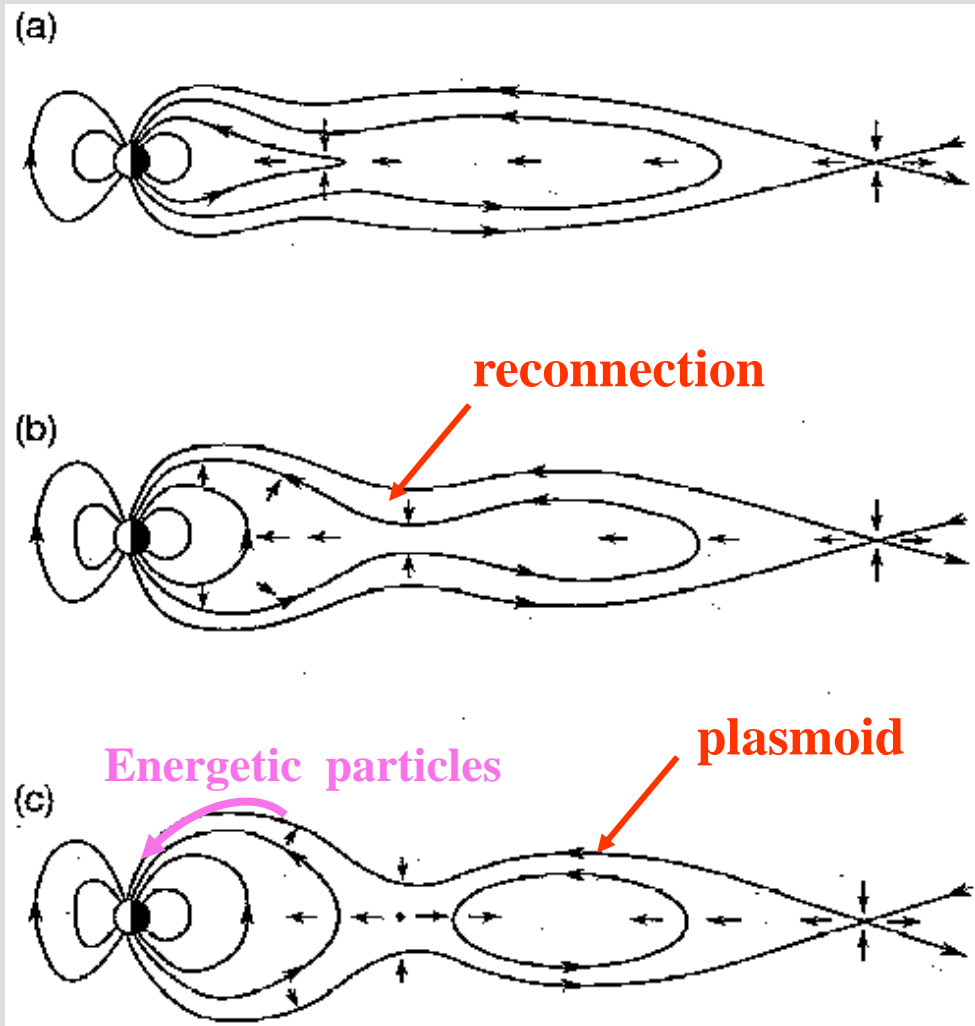




Aurora during substorm

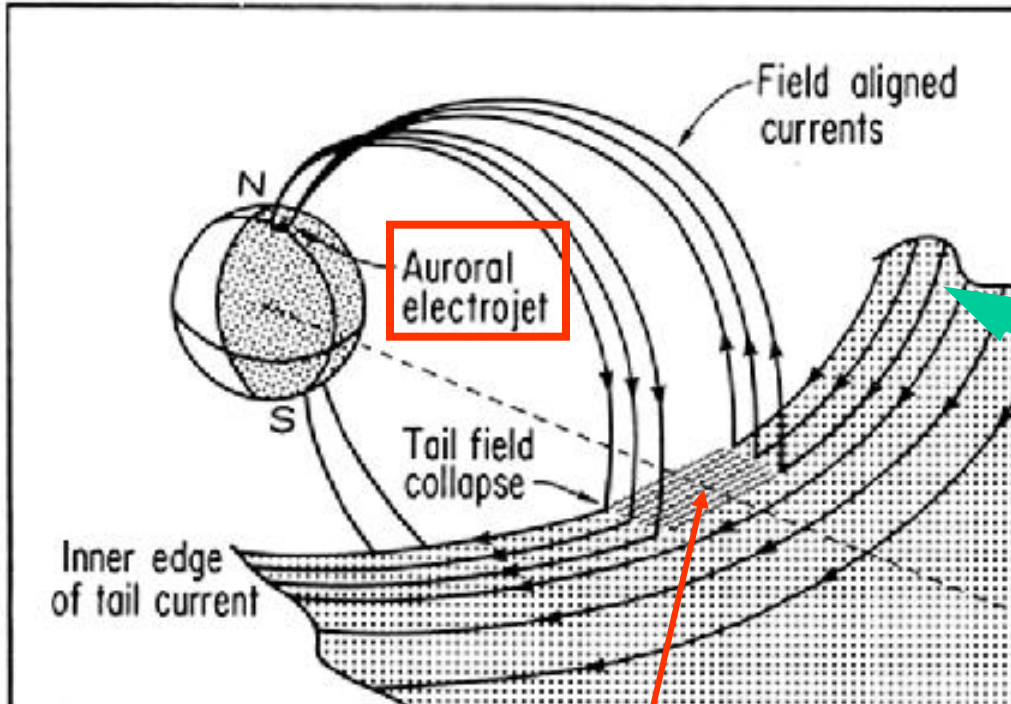


Substorms - magnetosphere



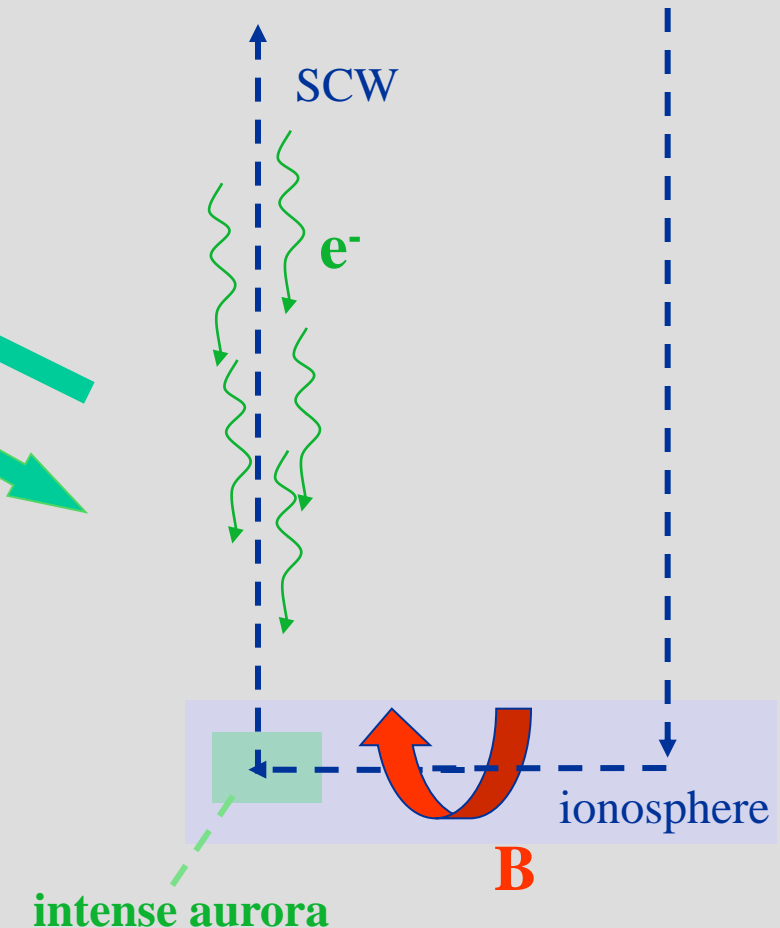
- **GROWTH PHASE:** When IMF southward, energy is pumped into magnetostail and is stored as magnetic energy
- **ONSET:** After a certain time (~ 1 h) the magnetostail goes unstable and “snaps” due to fast reconnection.
- **EXPANSION/MAIN PHASE:** Close to Earth the magnetosphere returns to dipole-like configuration. Plasma is energized and injected into the inner parts of the magnetosphere.
- **RECOVERY PHASE:** In the outer parts of the magnetotail a *plasmoid* is ejected. The magnetosphere returns to its ground state.

Substorm Current Wedge (SCW)



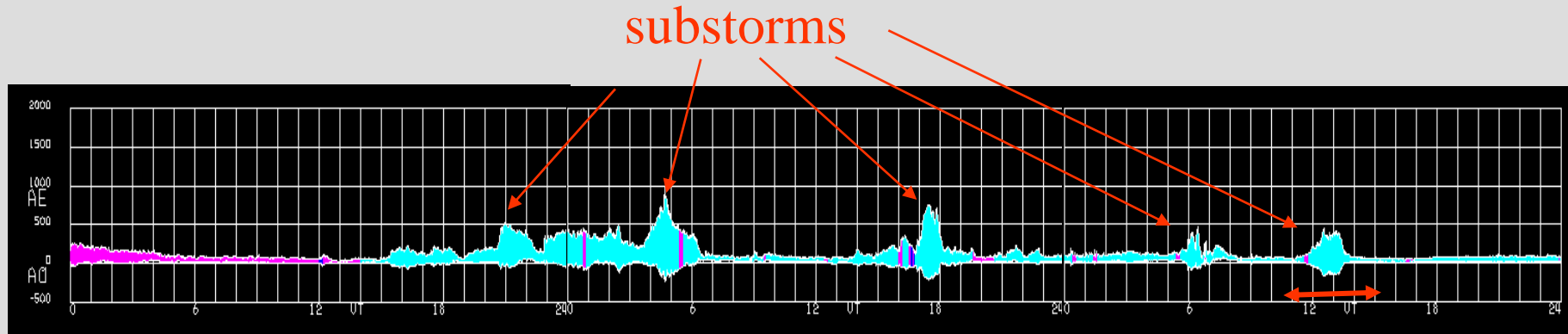
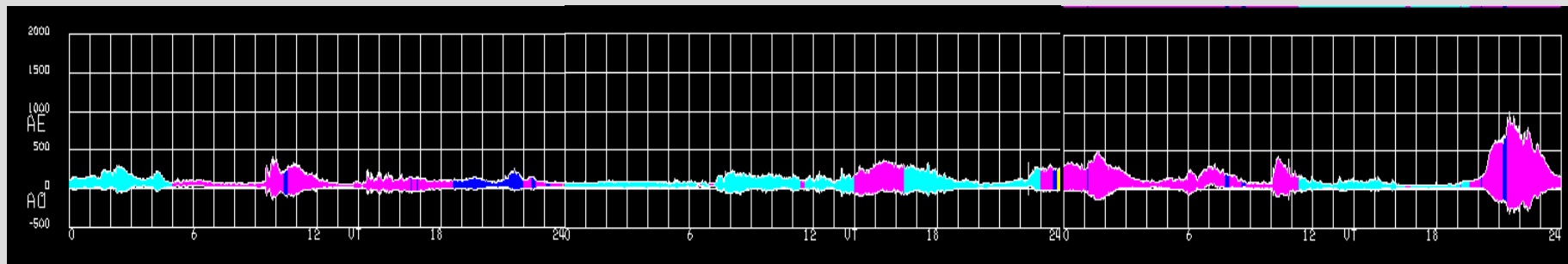
Due to reconnection processes the resistivity increases here
 \Rightarrow

Current takes another direction – through the ionosphere!



Auroral Electrojet (AE) index

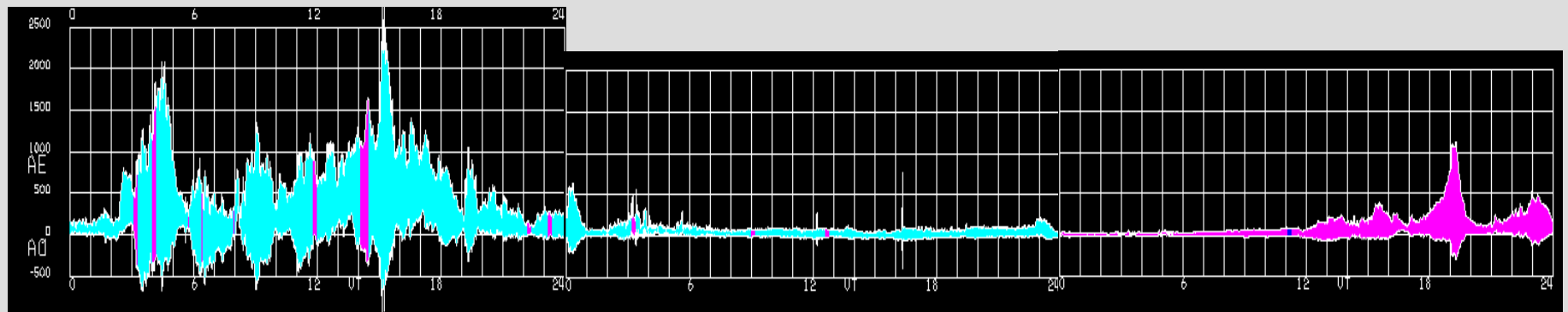
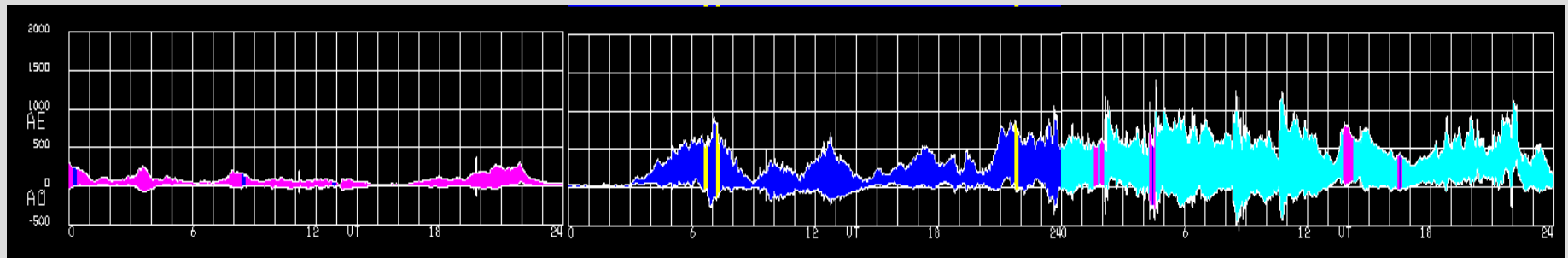
The AE index Measures the strength of the substorm current wedge (SCW), by using the information from several magnetic observatories.



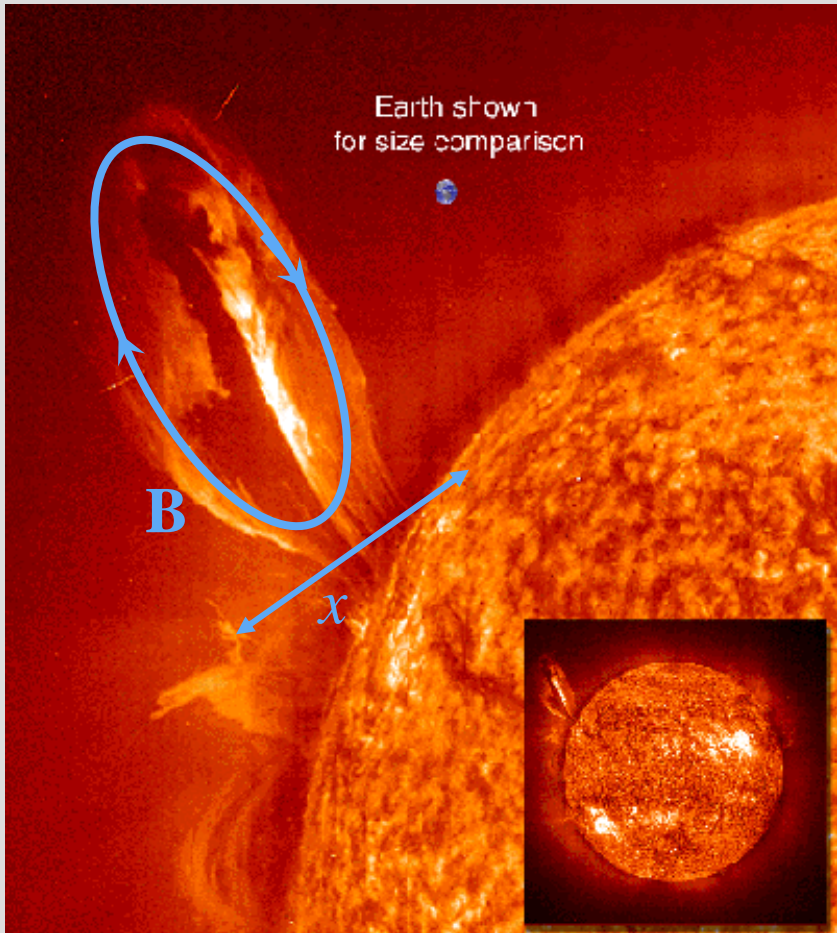
$\sim 1 - 3 \text{ h}$

Geomagnetic storms

Geomagnetic storms are extended periods with southward interplanetary magnetic field (IMF) and a large energy input into the magnetosphere.



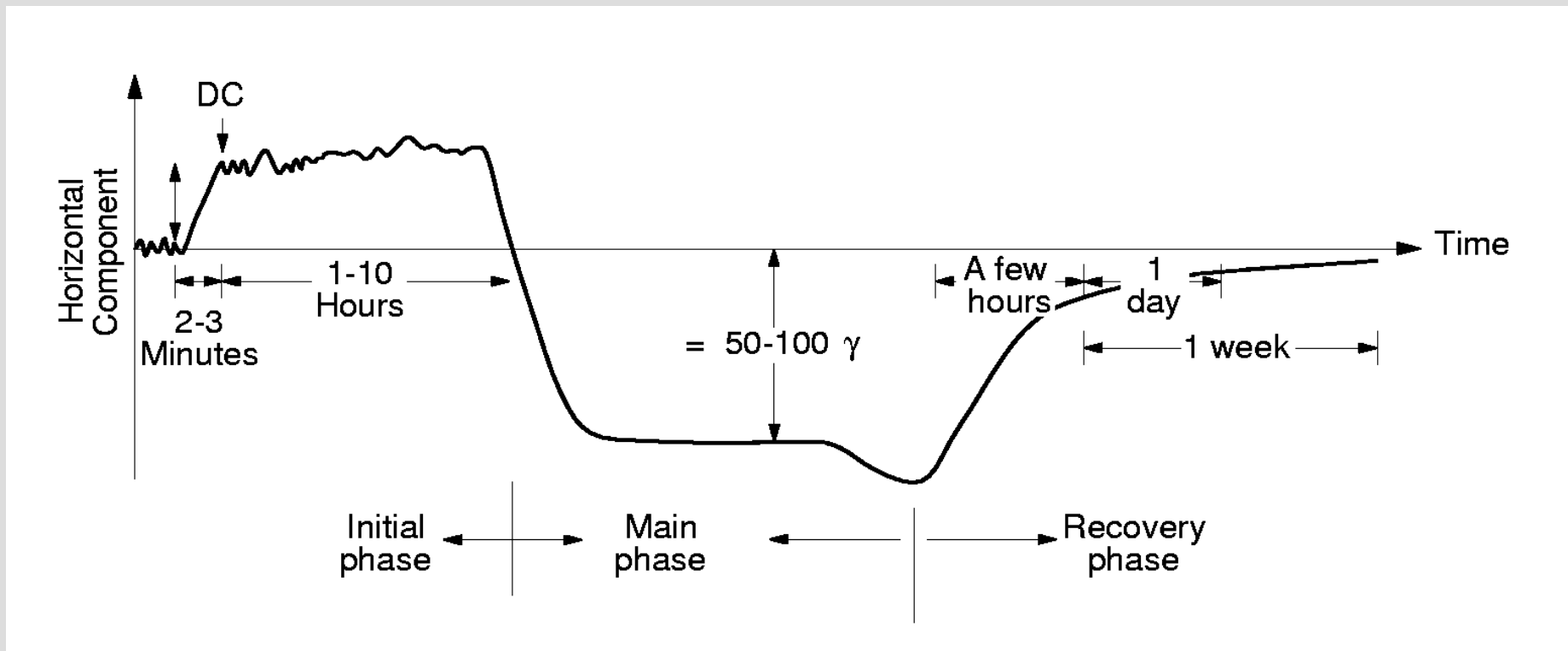
Geomagnetic storms and coronal mass ejections



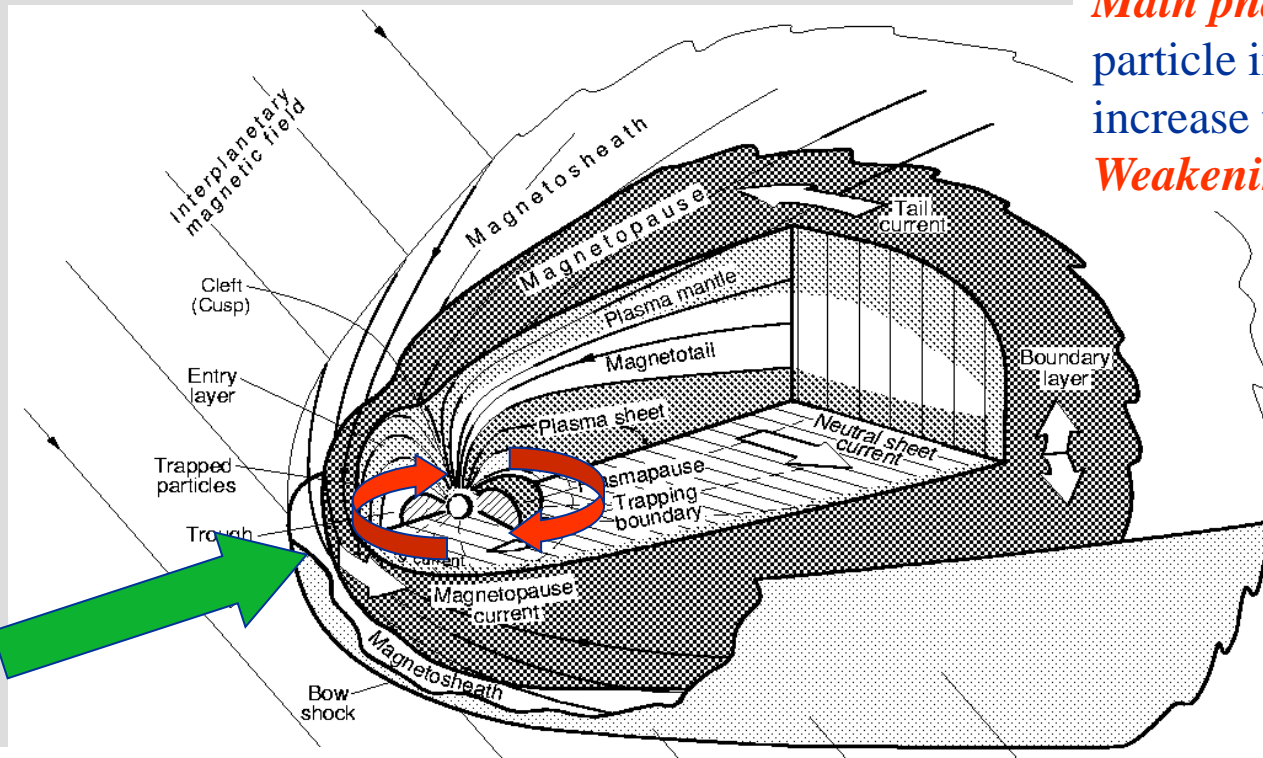
- Large geomagnetic storms are often associated with coronal mass ejections (CMEs)
- Because of their magnetic structure, they will give long periods with a constant IMF
- A typical time for a CME to pass Earth becomes $T = x/v \sim 10 R_E/1000 \text{ kms}^{-1} \sim 60 \text{ h}$

Geomagnetic storms - phases

Magnetogram



Geomagnetic storms - phases



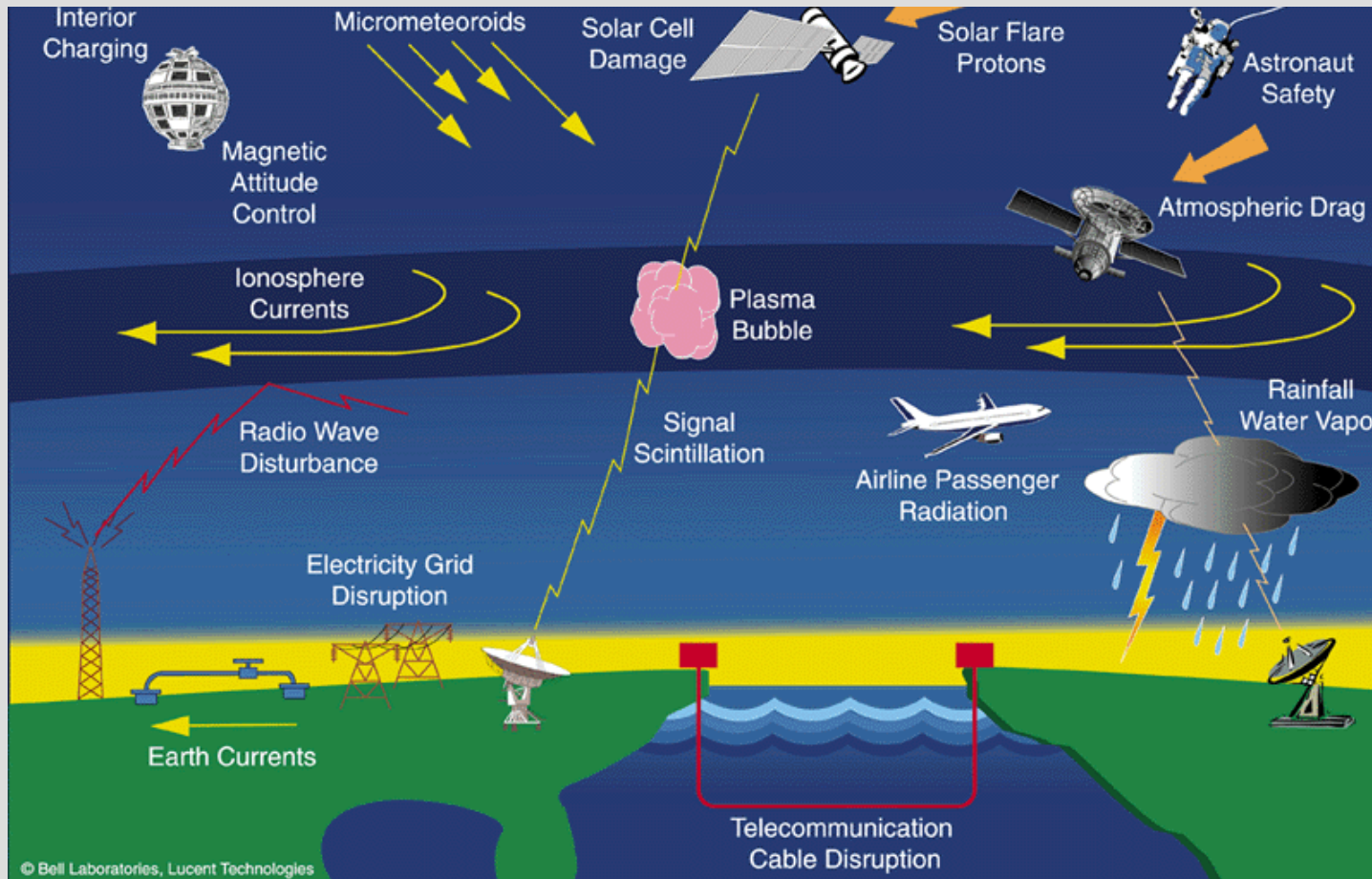
Initial phase: the magnetic cloud of the CME compresses the geomagnetic field.

Increase of B

Main phase: Several particle injections increase the ring current.
Weakening of B

Recovery phase: ring current returns to normal strength.
Recovery of B

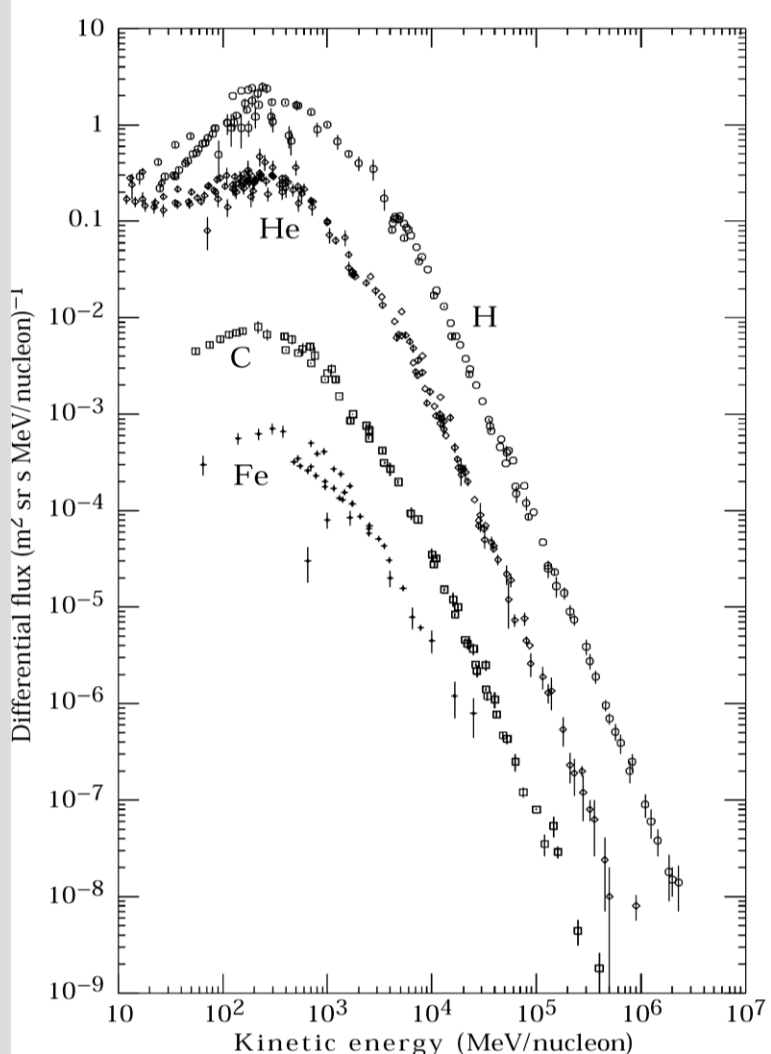
Space weather : consequences of solar and geomagnetic activity



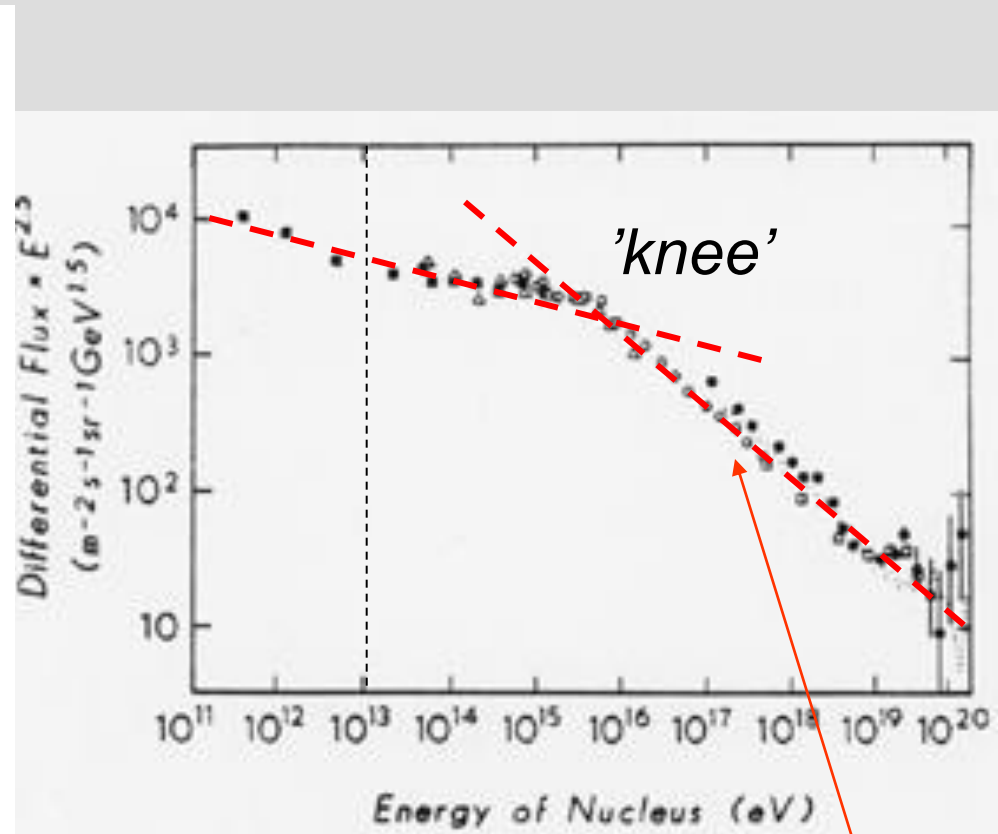
"conditions on the Sun and in the solar wind, magnetosphere, ionosphere and thermosphere that can influence the performance and reliability of space-borne and ground-based technological systems and can endanger human life or health."

US National Space Weather Programme

Spectrum of galactic cosmic radiation



Simpson, 1983.



Ultra-energetic cosmic radiation.
Origin unknown. Extragalactic???

Cosmic radiation

Primary cosmic radiation

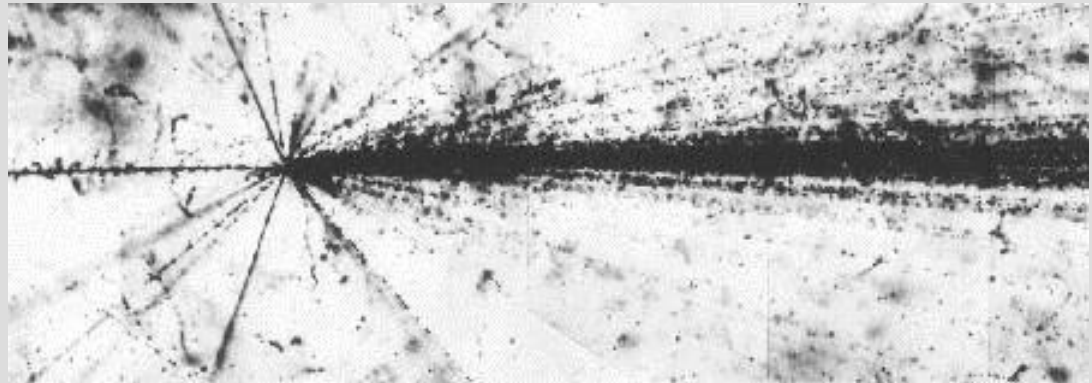
Extremely energetic particles ($>10^8$ eV) which originate outside of the solar system.

83 % protons

13 % alpha particles

3 % electrons

1 % other nuclei



Secondary cosmic radiation

- Starts at about 55 km altitude.
- Created by collisions between primary cosmic radiation and the atmosphere.
- Maximum (“*Pfotzer maximum*”) at approx. 20 km altitude.
- Contains mostly protons, neutrons and mesons

Pfotzer maximum

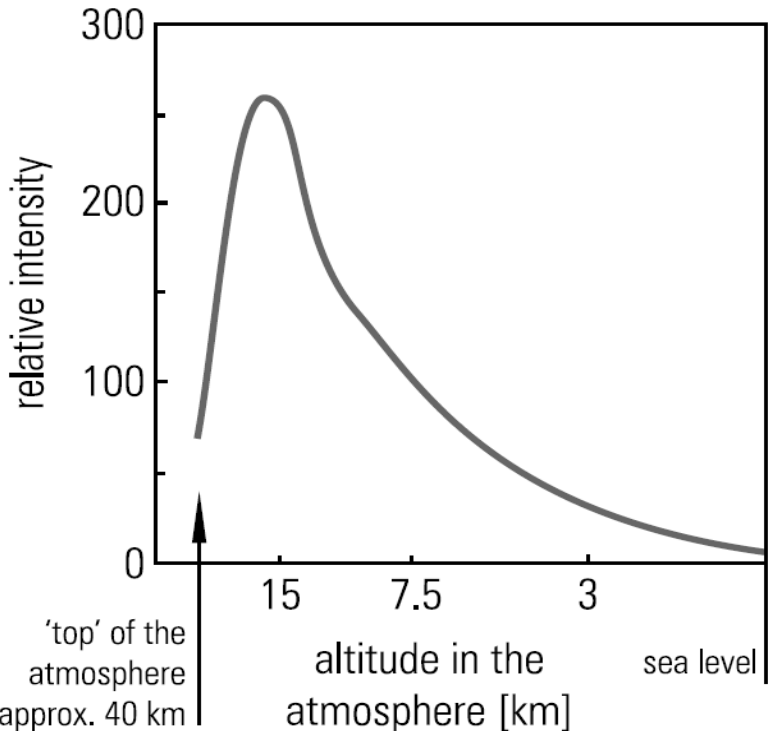
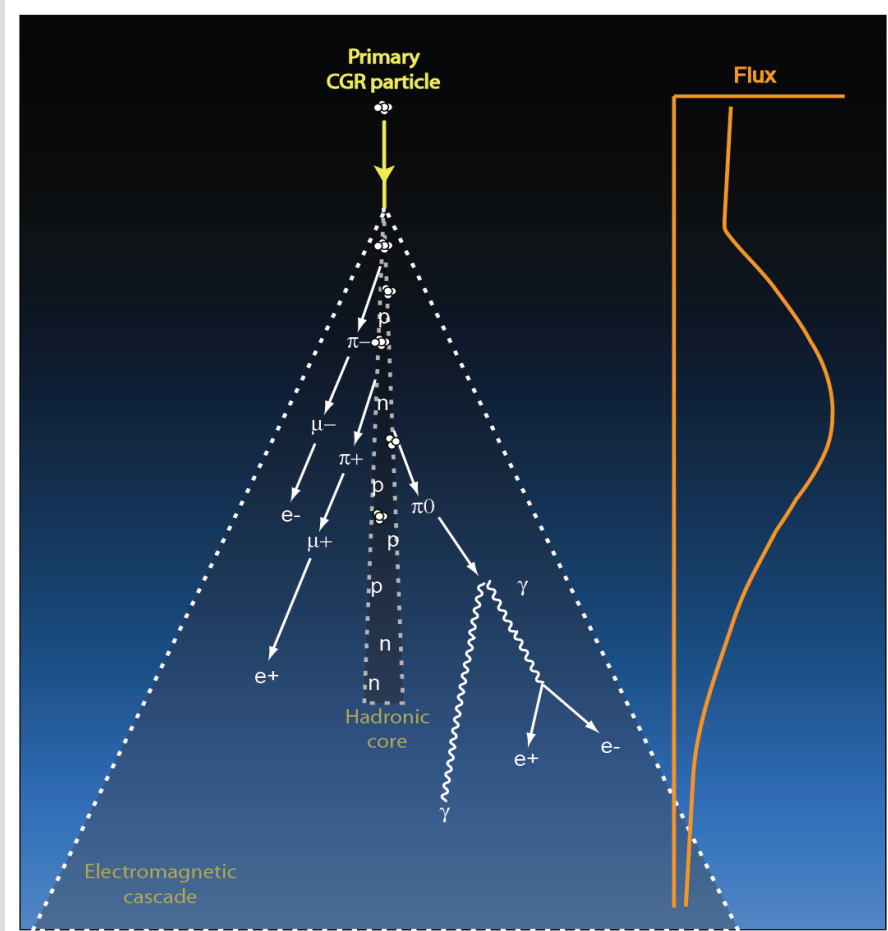
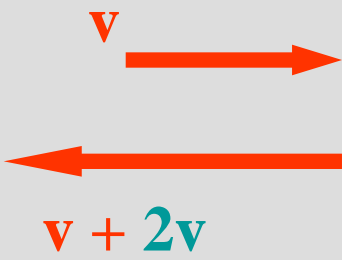


Fig. 1.12
Intensity profile of cosmic particles
in the atmosphere

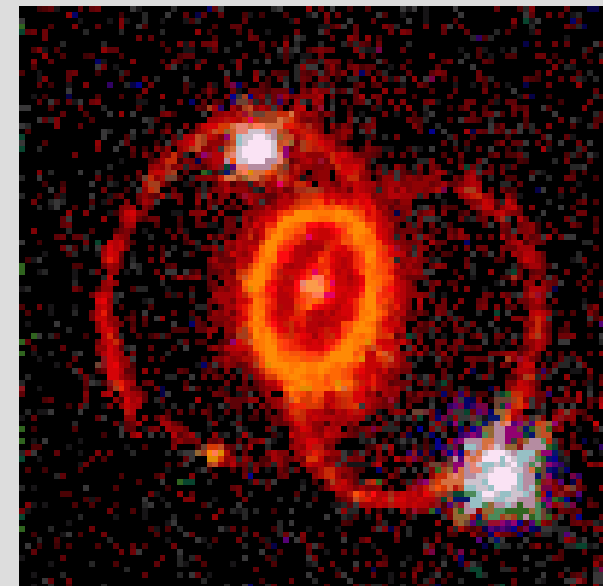


Origin of galactic cosmic radiation

Two main theories



Fermi acceleration
by two magnetic
mirrors in motion



Shock waves from
supernova explosion



Relativistic dynamics

Relativistic momentum

$$\mathbf{p} = \frac{m\mathbf{v}}{\sqrt{1 - \frac{v^2}{c^2}}} = \gamma m\mathbf{v}$$

$$\gamma \equiv \frac{1}{\sqrt{1 - \frac{v^2}{c^2}}}$$

Relativistic energy

$$E = \frac{mc^2}{\sqrt{1 - \frac{v^2}{c^2}}} = \gamma mc^2$$

Relation between energy and momentum

$$E^2 = p^2 c^2 + m^2 c^4$$

Relativistic dynamics

Rest energy

$$E = mc^2$$

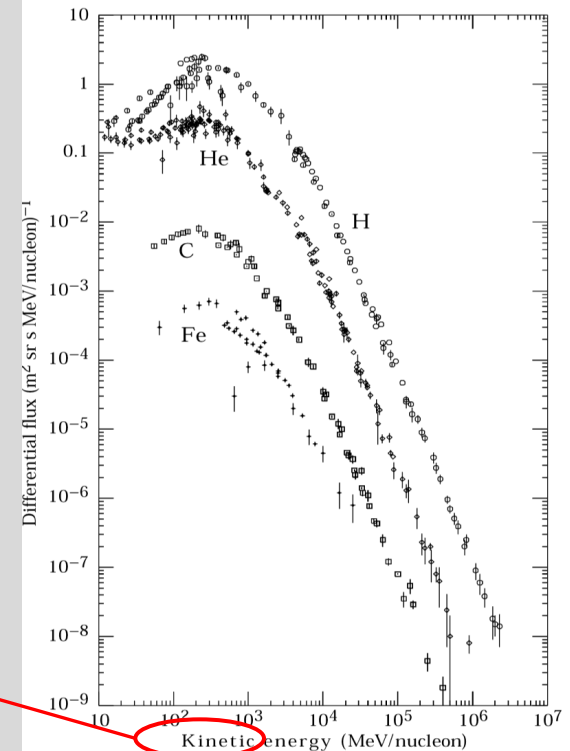
Kinetic energy

$$E_{kin} = E - mc^2 = mc^2(\gamma - 1)$$

Rest energy of electron: 512 keV \sim 0.5 MeV

Rest energy of proton: 939 MeV \sim 1 GeV

!!!



24.1: Major components of the primary cosmic radiation (from Ref. 1).



Relativistic gyro radius

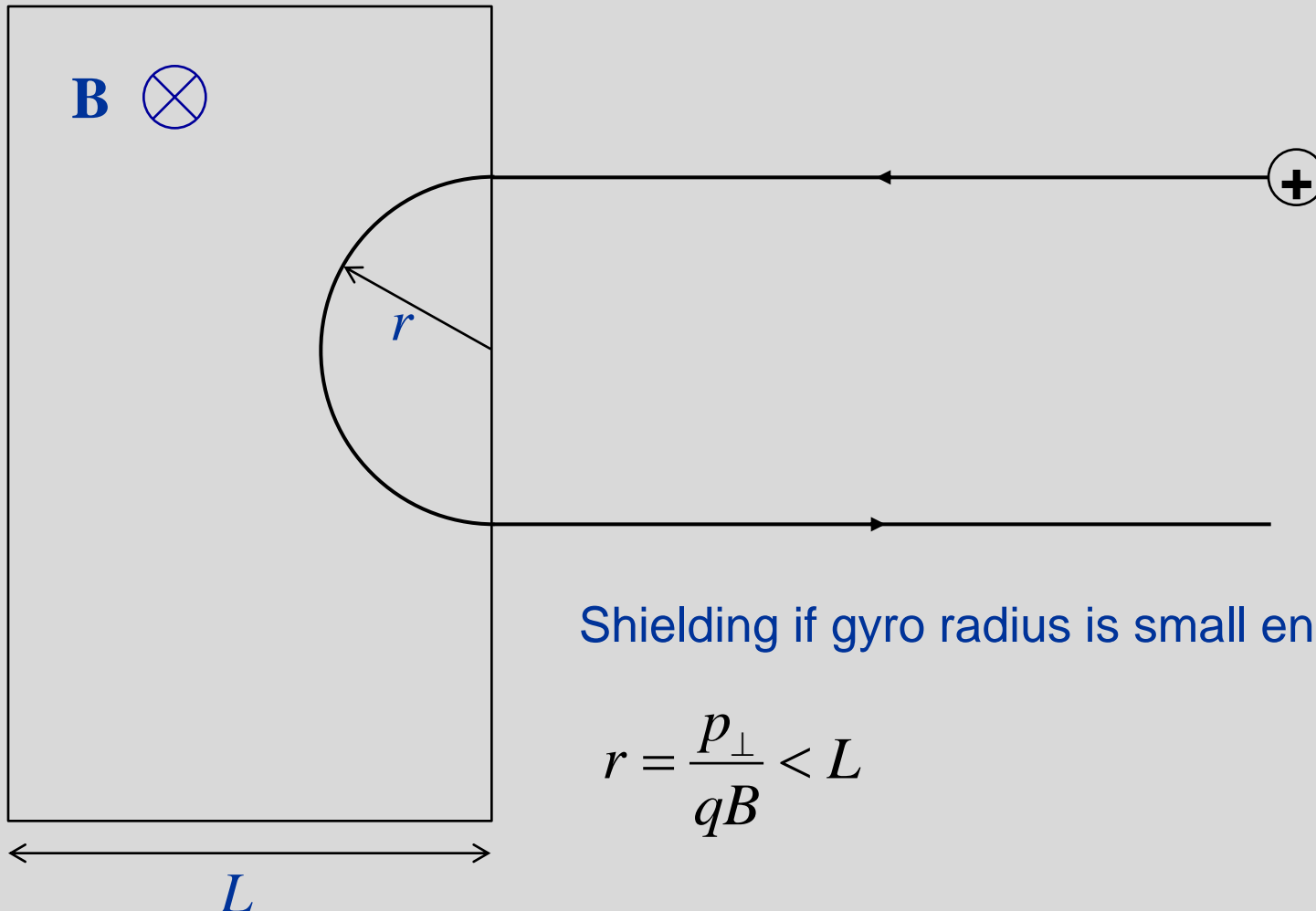
Non-relativistic
gyro radius

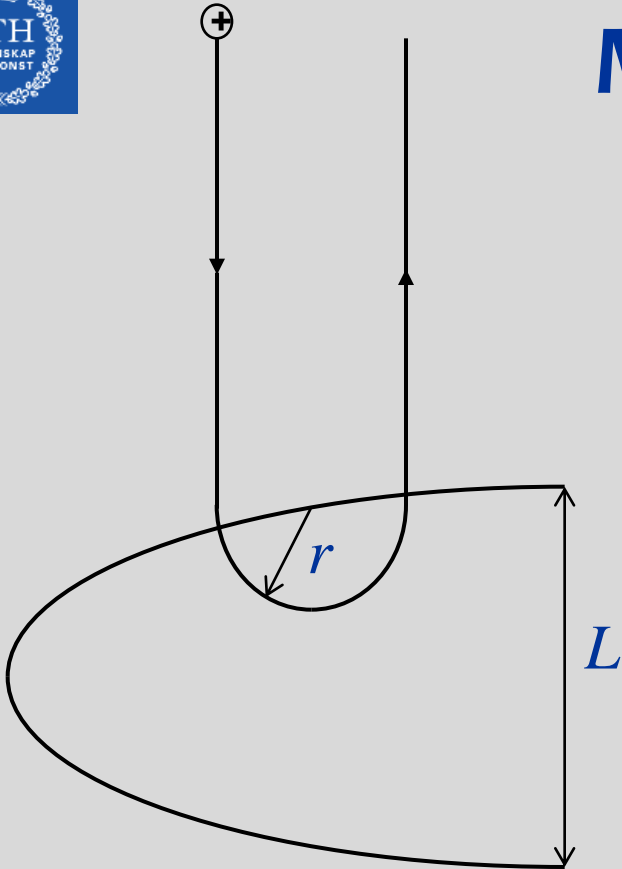
$$r_L = \frac{mv_\perp}{qB} = \frac{p_\perp}{qB}$$

Relativistic
gyro radius

$$r_L = \frac{p_{rel,\perp}}{qB} = \gamma \frac{mv_\perp}{qB}$$

Magnetic shielding





Magnetic shielding of magnetosphere

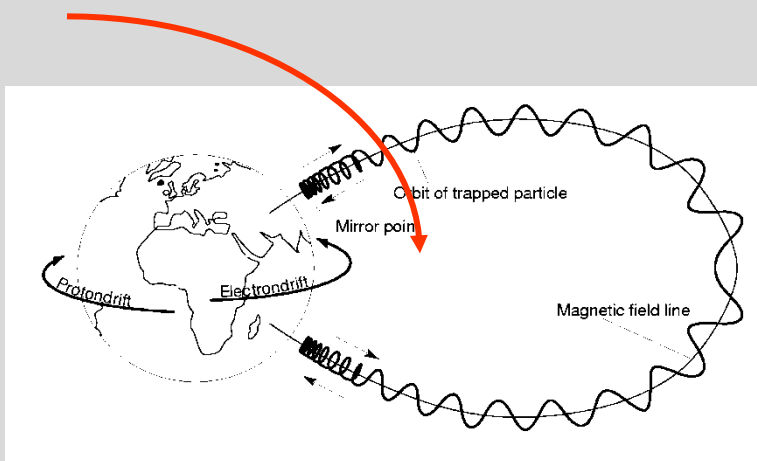
Shielding if

$$r = \frac{p_{\perp}}{qB} < L$$

What will be the maximum energy of cosmic ray particles that will be shielded?

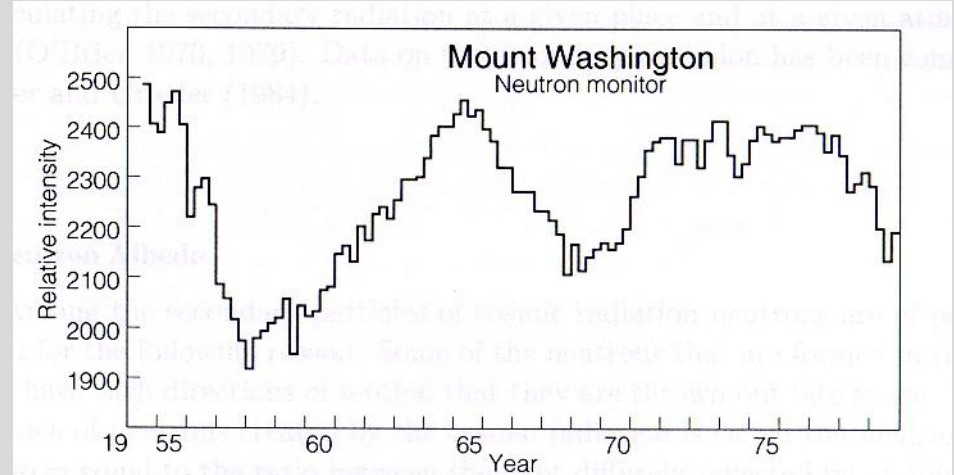
Effect of magnetic field

- Cosmic radiation is affected by magnetic field, as all the smaller the gyro radius, the more difficult it is for the particle to reach Earth.



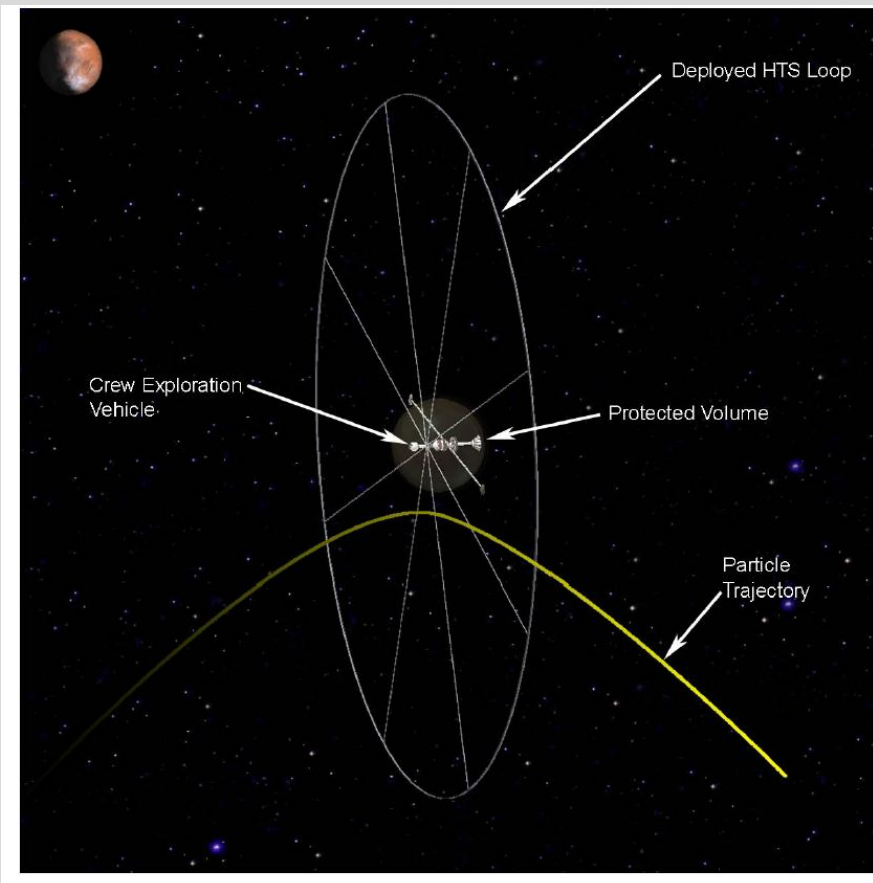
- Gyro radius is $r = p/(eZB)$.
Define rigidity:

$$P = pc/(eZ)$$



- Temporal variations:
 - 27 days (IMF, solar rotation)
 - 11 years (IMF, solar cycle)

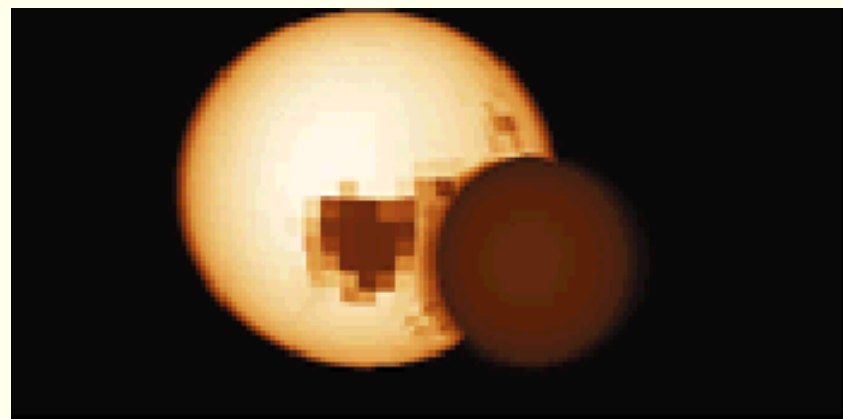
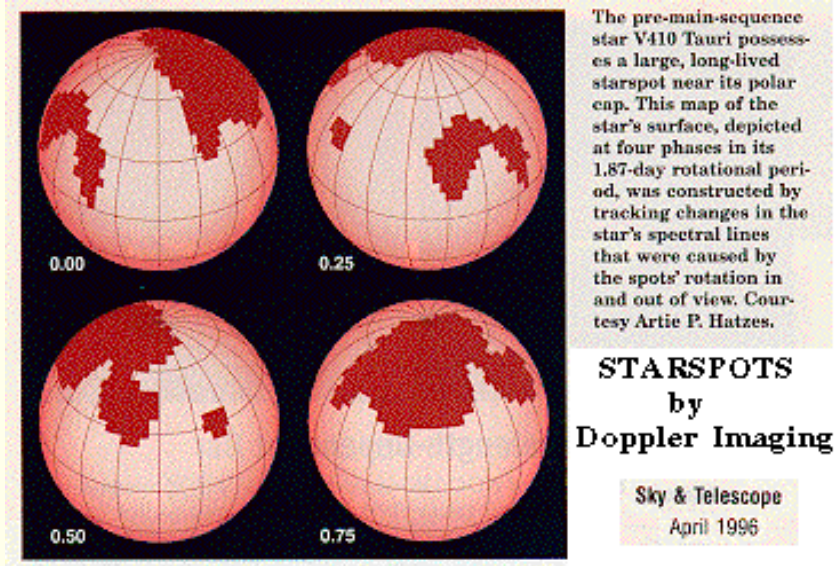
Artificial magnetic shielding of spacecraft





Plasma outside of the solar system

Starspots

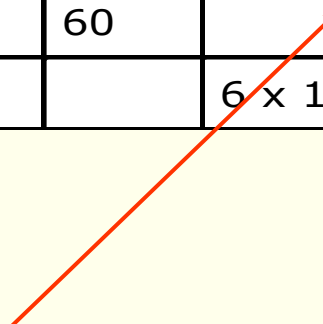


Eclipse mapping, XY Ursae Majoris

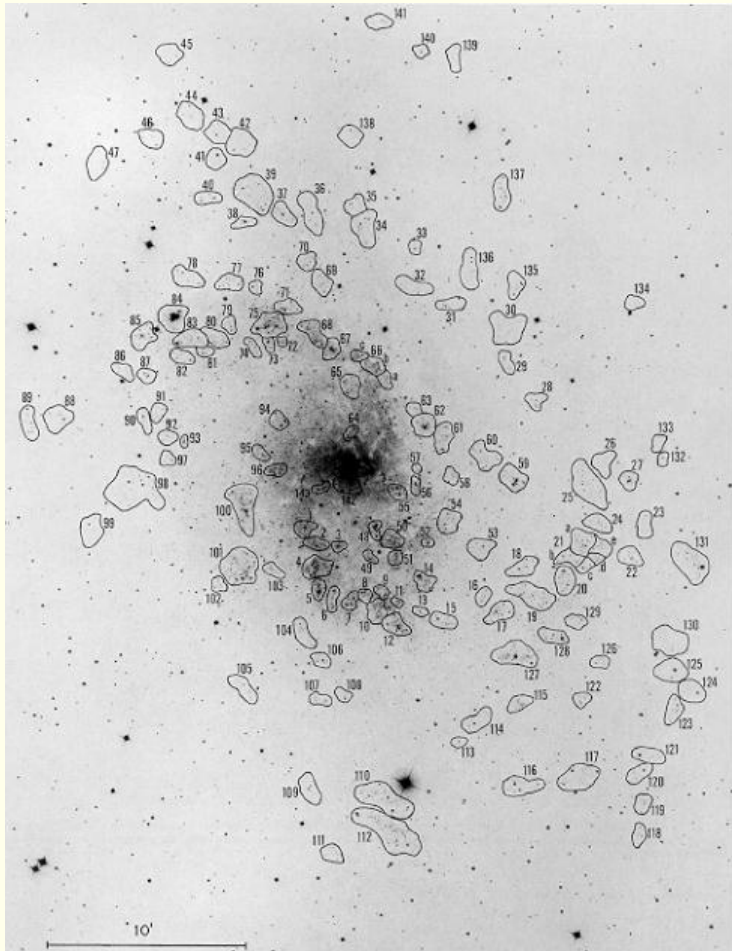
Stellar winds

Star	Type	Mass (M_{\odot})	M-dot (M_{\odot}/yr)	v_{∞} (km/s)
α Sco (Antares)	M1.5 Iab-Ib	15	1×10^{-6}	17
<u>Sun</u>	G2V	1	1×10^{-14}	200 – 700
<u>ζ Pup</u> (Naos)	O4I(n)f	59	2.7×10^{-6} 2.4×10^{-6}	– 2,200
<u>P Cyg</u>	"B0Ia" (<u>LBV</u>)	30-60	1.5×10^{-5}	210
WR1	WN5 (<u>W-R</u>)		6×10^{-5}	2,000

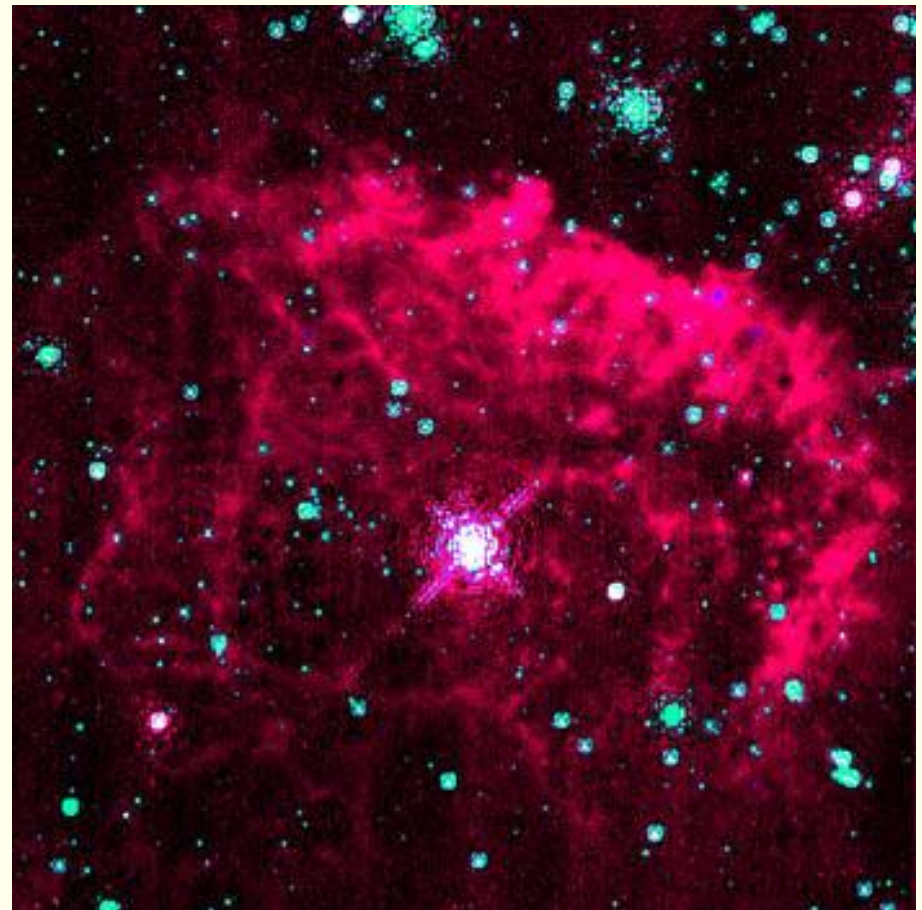
~20 % of the mass during the star's life time



Stellar winds



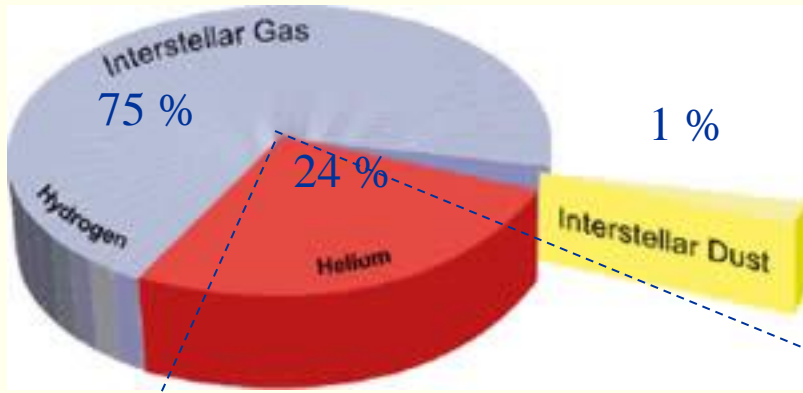
Doppler measurements of stellar winds



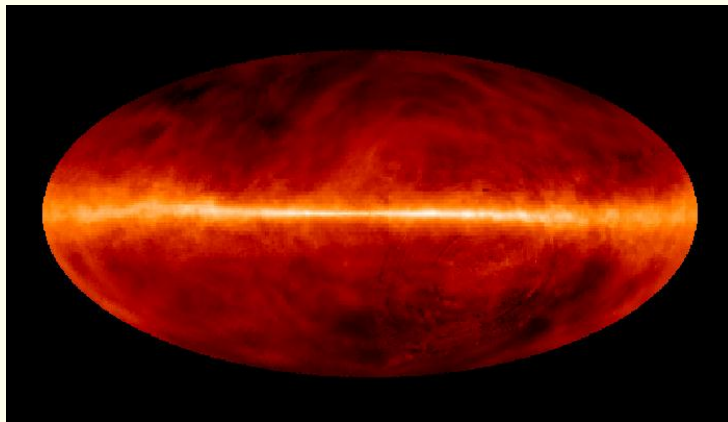
Pistol nebula – probably created by massive outflow of stellar plasma

Interstellar plasma

Interstellar matter (10 % of Milky Way mass)



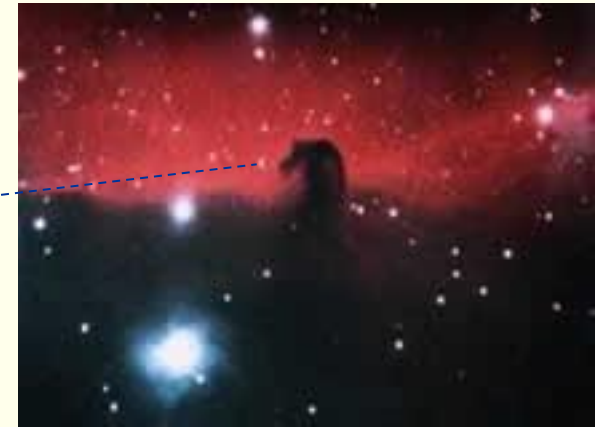
H I regions (neutral hydrogen)



H II regions
(emission nebulae)



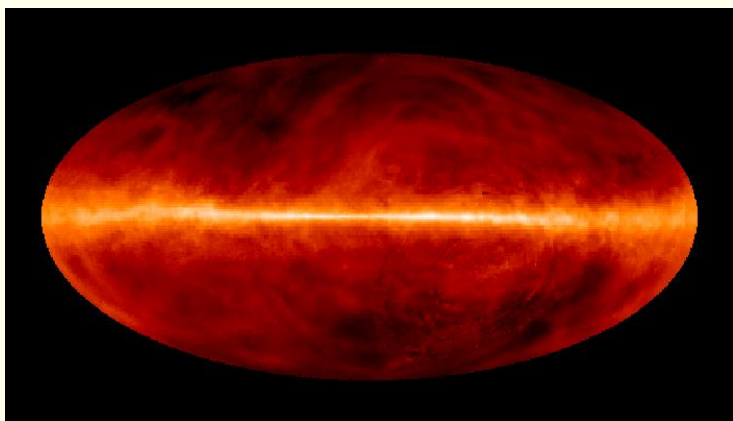
Horsehead nebula



Trifid nebula

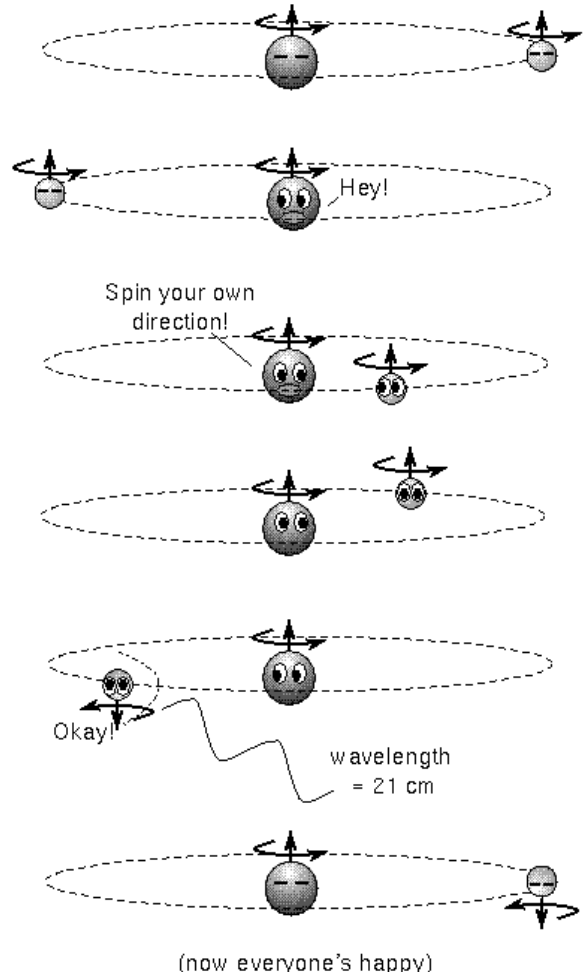
H_I regions

- Not reached by UV radiation from stars
- Either diffuse or concentrated as interstellar clouds
- Mostly contains unionized hydrogen, but also some ionized Ca
- Density of diffuse part is $0.1 - 50 \text{ cm}^{-3}$
- Ionization degree $\sim 0.01 \%$
- $T \sim 50 - 100 \text{ K}$
- $B \sim 0.1 \text{ nT}$



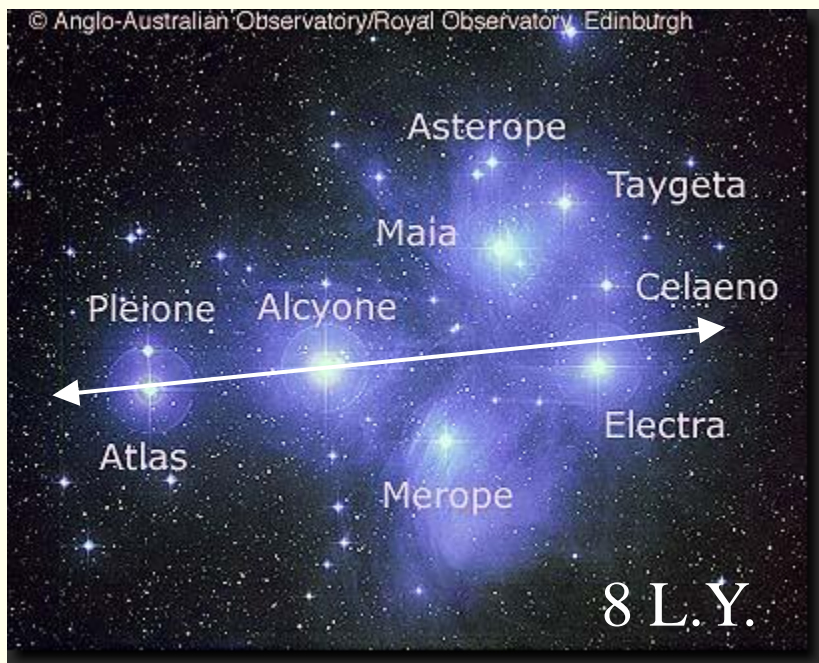
Distribution of interstellar H I gas in the Northern sky, observed at the 21 cm radio spectral line.

Neutral atomic Hydrogen creates 21 cm radiation



H₂ regions are reservoirs of material for star formation

Stars are formed by gravitational collapse of interstellar clouds



Pleiades cluster

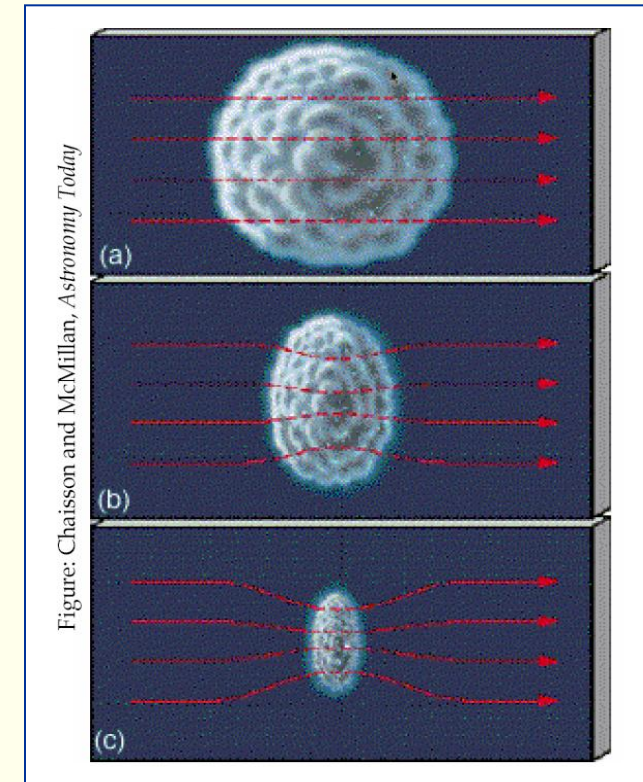
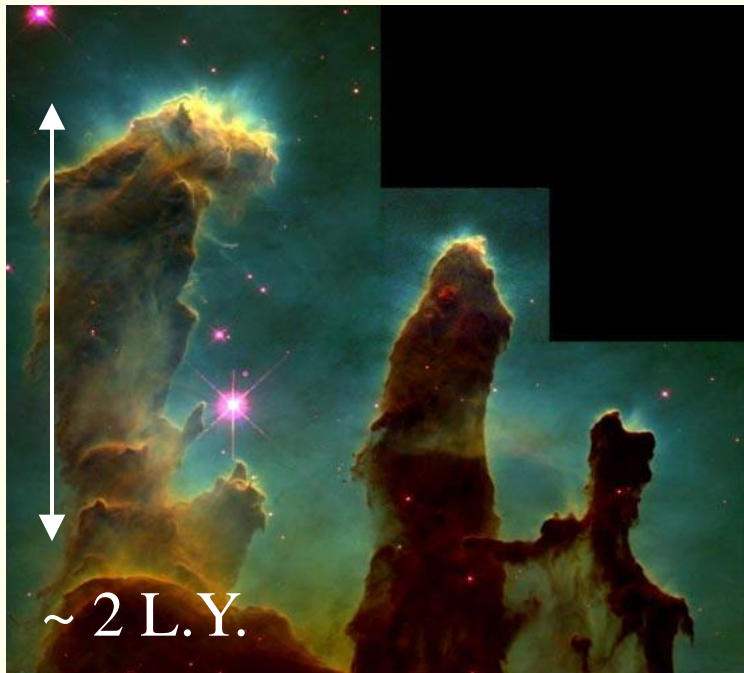
Closeup of region close to Merope



The emissions are caused by reflection by the dust particle component of the clouds.

H₁ regions are reservoirs of material for star formation

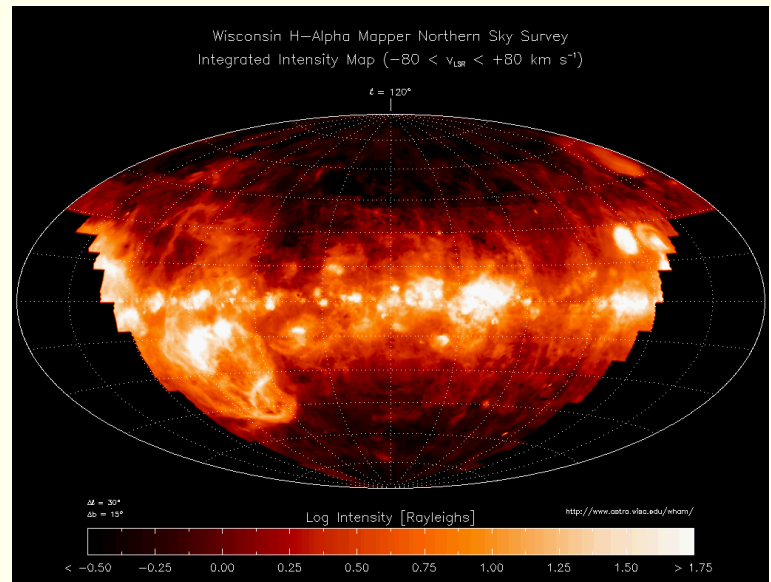
The interstellar medium is turbulent, and localized density enhancements (clouds) are often created. These may contain molecular Hydrogen and dust.



The small ionized part of the cloud can collapse more easily along B than across it, because of the gyro motion, creating a pancake form. Centrifugal forces may also be important.

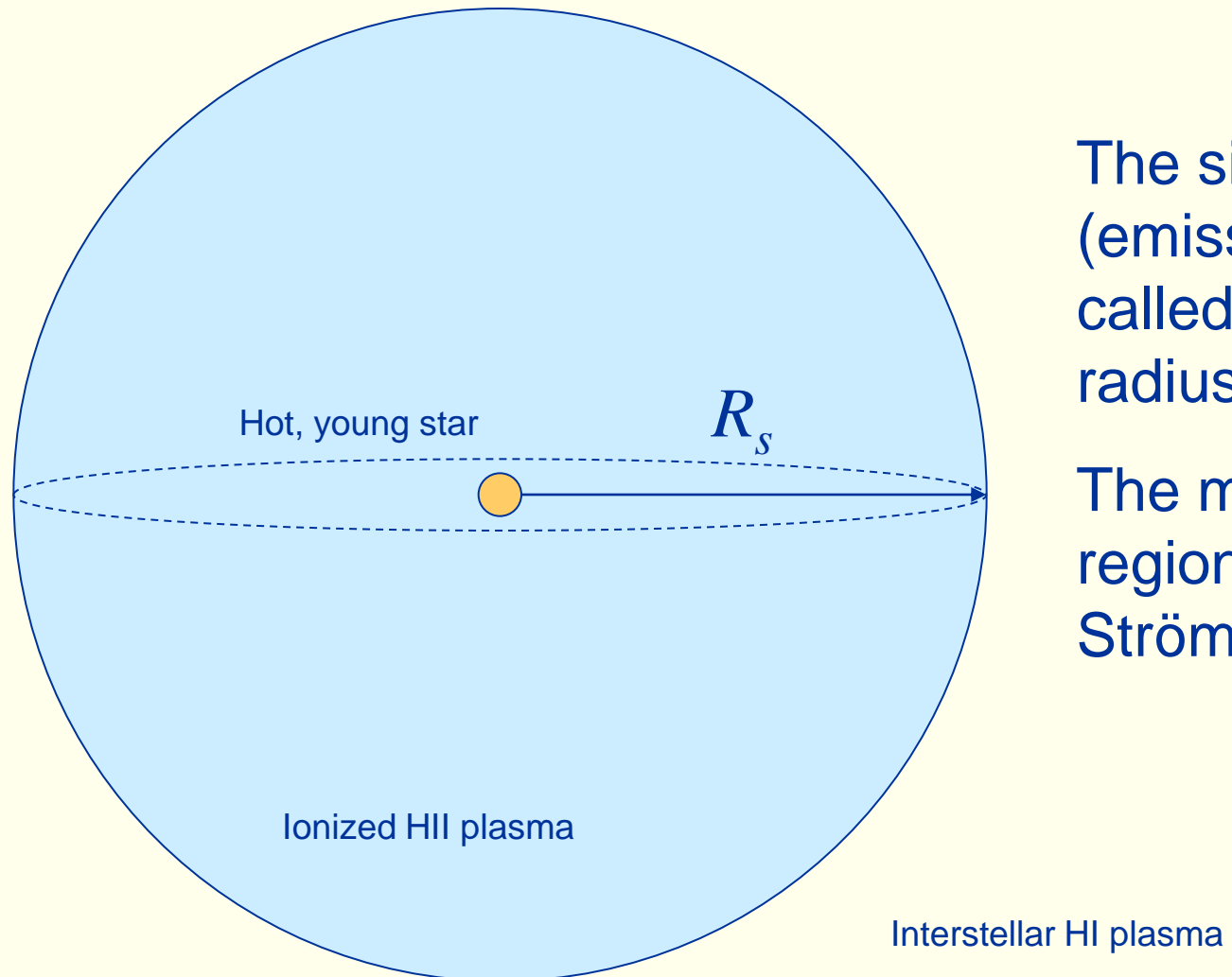
Interstellar plasma – HII regions

- Reached by UV radiation by young hot stars.
- Mostly contains ionized hydrogen
- Approx. same density as HI regions.
- Ionization degree $\sim 100\%$
- $T \sim 10\,000\,K$
- $B \sim 1\,nT$



Distribution of interstellar HII gas in the Northern sky

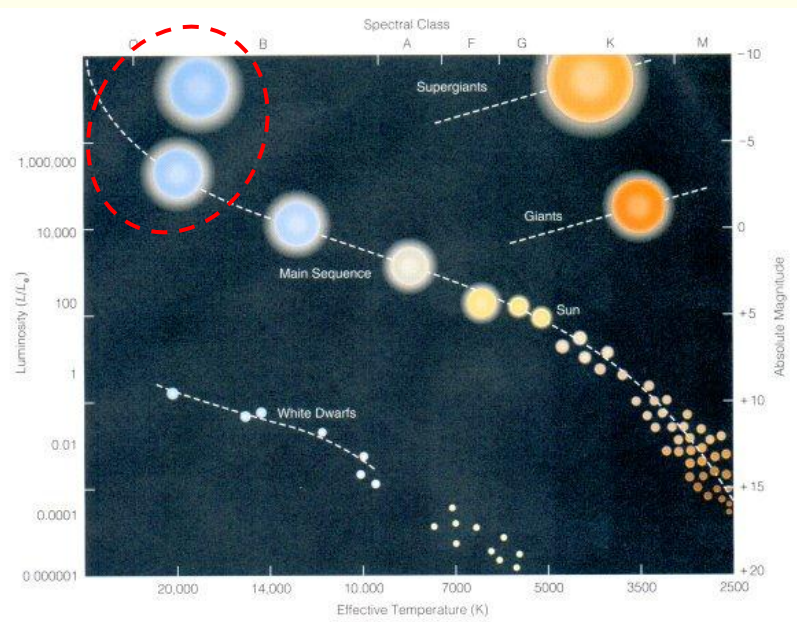
Strömgren sphere



The size of the HII region (emission nebula) is called the Strömgren radius, R_s .

The modelled, spherical region is called a Strömgren sphere.

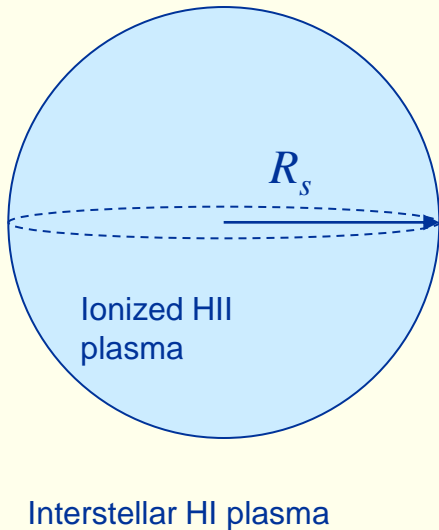
Strömgren sphere



Herzsprung-Russel diagram

- A hot star ($> 30\,000$ K) emits significant numbers of photons with energy > 13.6 eV (ionization energy for HI) $\leftrightarrow \lambda < 912$ Å = EUV radiation
- The star emits N_{UV} photons/s
- Interstellar plasma originally contains n_0 HI atoms
- The absorption cross section of HI is very high, so EUV radiation is quickly absorbed and we can assume 100 % ionization ratio.

Strömgren radius



- The recombination rate inside the Strömgren radius is

$$r = \alpha_H n_e n_p = \alpha_H n_e^2 = \alpha_H n_H^2$$

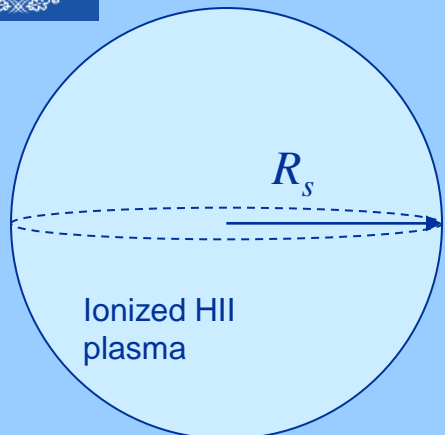
- In equilibrium, we have

$$N_{UV} = rV = \alpha_H n_H^2 \frac{4\pi R_s^3}{3} \Rightarrow$$

$$R_s = \left(\frac{3N_{UV}}{4\pi\alpha_H n_H^2} \right)^{1/3}$$

Hotter star
 Denser gas

Strömgren radius



N_{UV} can be determined by considering black-body radiation properties of the star (Temperature and surface area). For a hot, young star it can be $\sim 10^{49} \text{ s}^{-1}$. For a typical HII density of $n_H = 35 \text{ cm}^{-3}$, what is the Strömgren radius in light years?

$$\alpha_H \approx 3 \times 10^{-13} \text{ cm}^3 \text{s}^{-1}$$

$$R_s = \left(\frac{3N_{UV}}{4\pi\alpha_H n_H^2} \right)^{1/3}$$

Blue

0.2 L.Y.

Yellow

2000 L.Y.

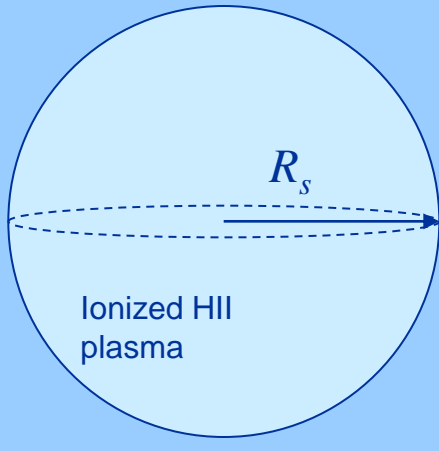
Red

20 L.Y.

Green

2×10^5 L.Y.

Strömgren radius



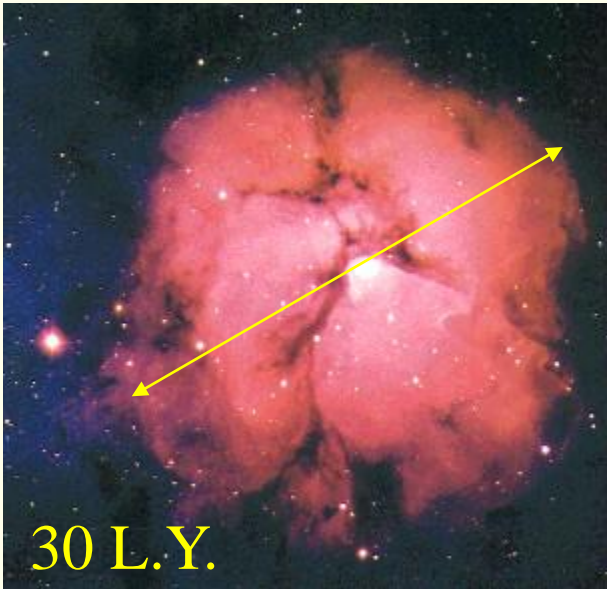
N_{UV} can be determined by considering black-body radiation properties of the star (Temperature and surface area). For a hot, young star it can be $\sim 10^{49} \text{ s}^{-1}$. For a typical HI density of $n_H = 35 \text{ cm}^{-3}$, we get

$$\alpha_H \approx 3 \times 10^{-13} \text{ cm}^3 \text{s}^{-1}$$

Red

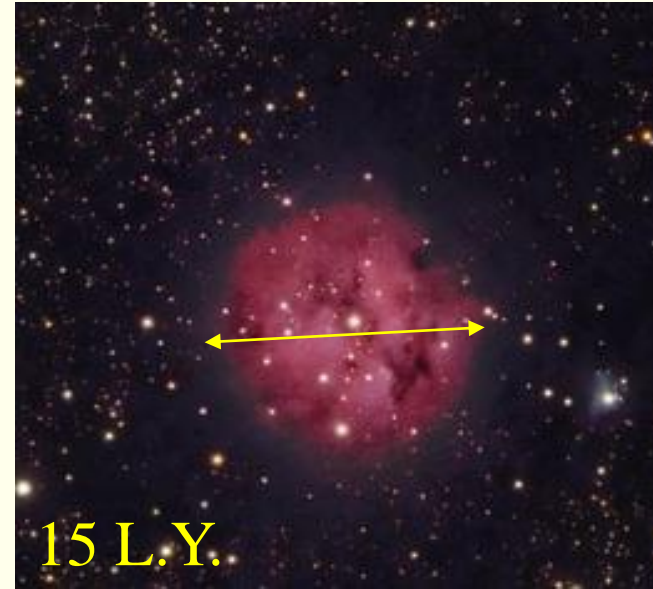
$$R_s = \left(\frac{3N_{UV}}{4\pi\alpha_H n_H^2} \right)^{1/3} = \left(\frac{3 \cdot 10^{49}}{4\pi \cdot 3 \cdot 10^{-19} \cdot (3.5 \cdot 10^7)^2} \right)^{1/3} = 1.9 \cdot 10^{17} \text{ m} = 20 \text{ L.Y.}$$

Emission nebulae



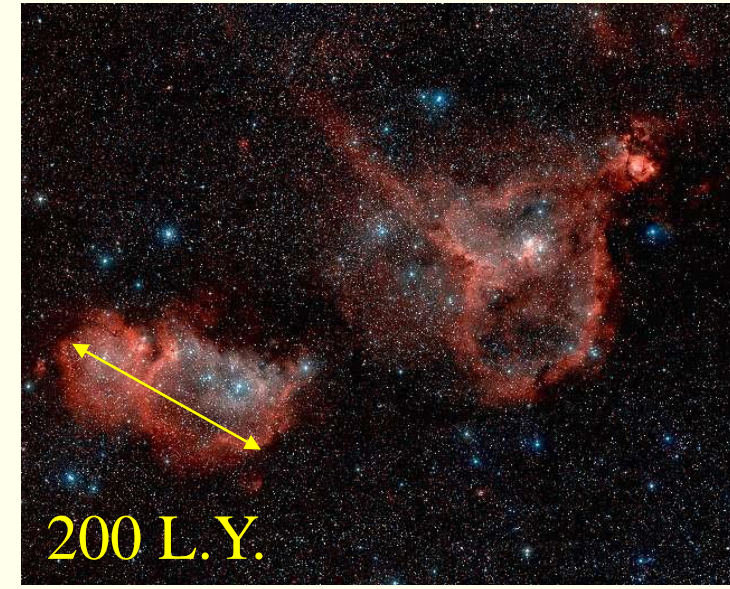
30 L.Y.

Trifid nebula (Messier 20)



15 L.Y.

IC5146



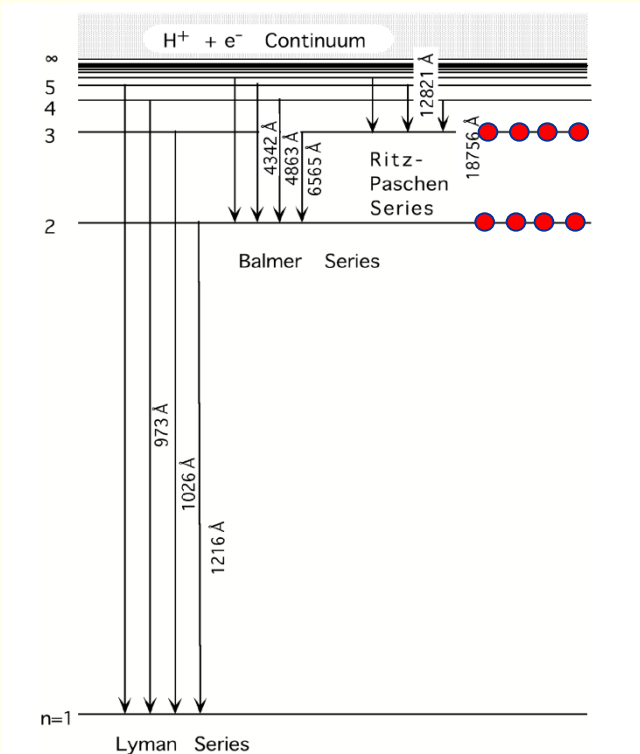
200 L.Y.

Heart and Soul nebulae
(IC1805, IC1848)

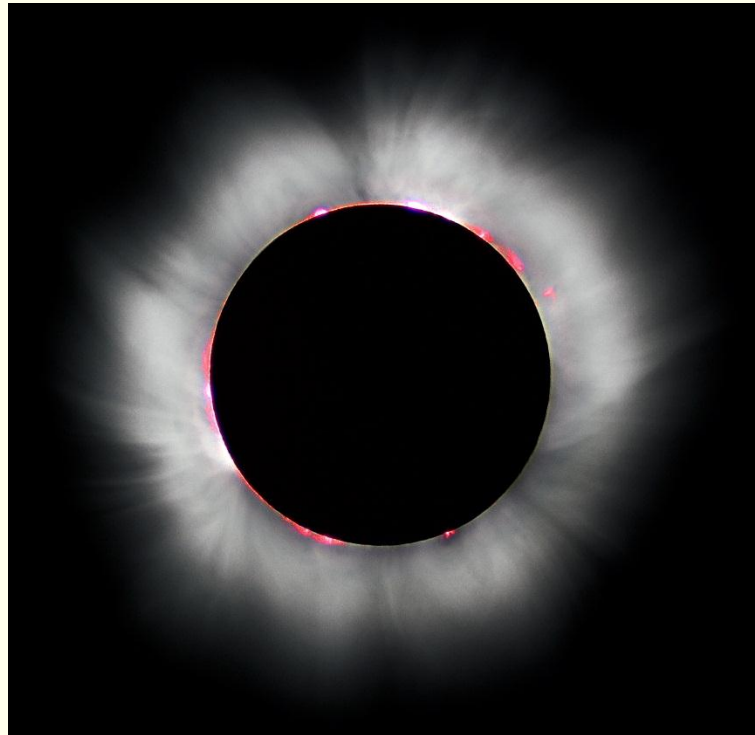
- Emission nebulae often appear red, due to a prominent emission in the Balmer series
- May be non-spherical due to
 - *Gradients in the background medium*
 - *Multiple stars at the core*

Why is the chromosphere red?

Hydrogen spectrum



T_2
 T_1



Interstellar magnetic field

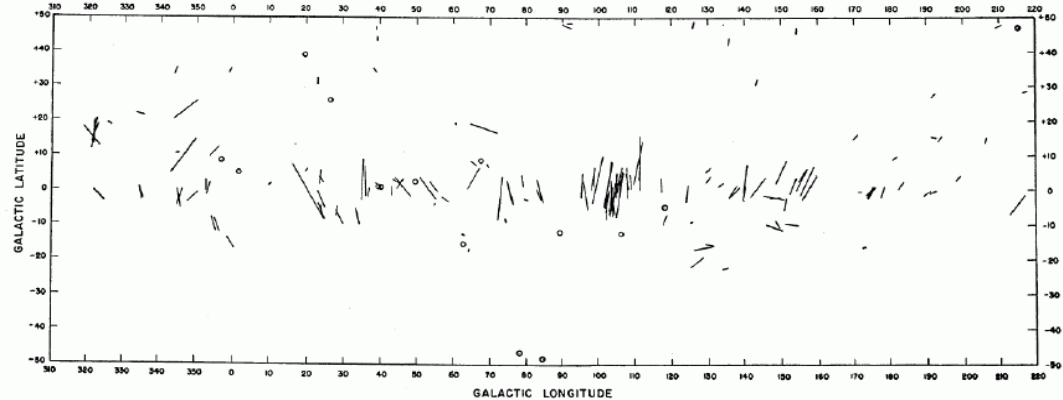


Figure 1. Vector diagram showing polarization of individual stars.

Hall & Mikesell, 1949, AJ, 54, 187

HI regions: ~ 0.1 nT

HII regions: ~ 1 nT

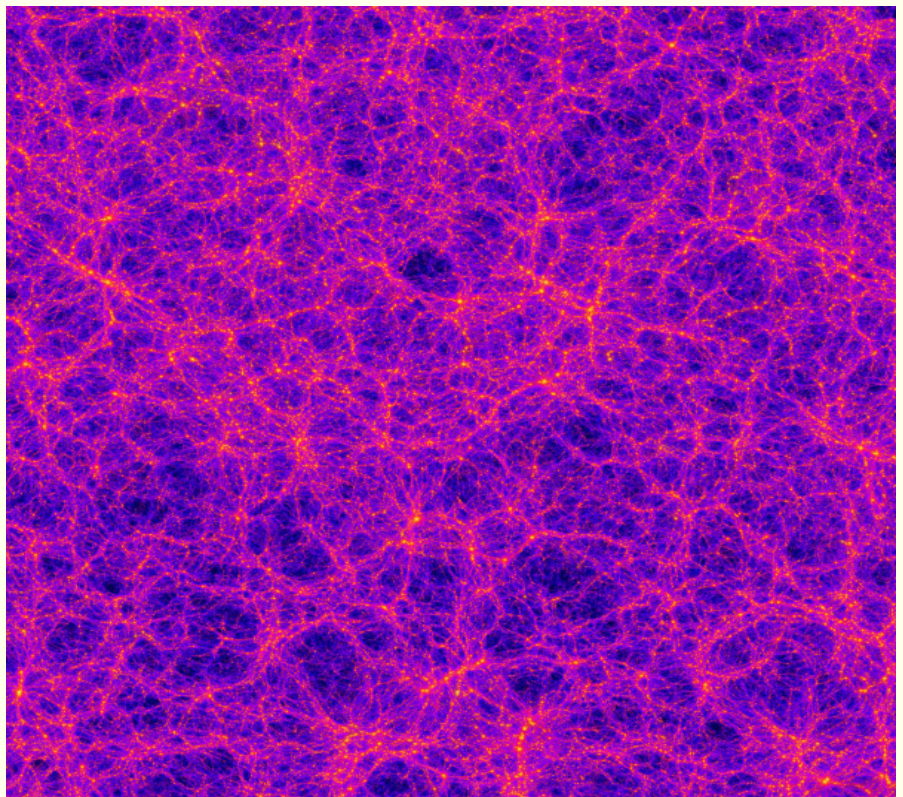
Magnetic field important also in the interstellar medium!

Intergalactic matter



Interacting Galaxies NGC 1409 and NGC 1410
Hubble Space Telescope • STIS

$2.7 \cdot 10^9$ light years



Computer simulation of intergalactic mass distribution



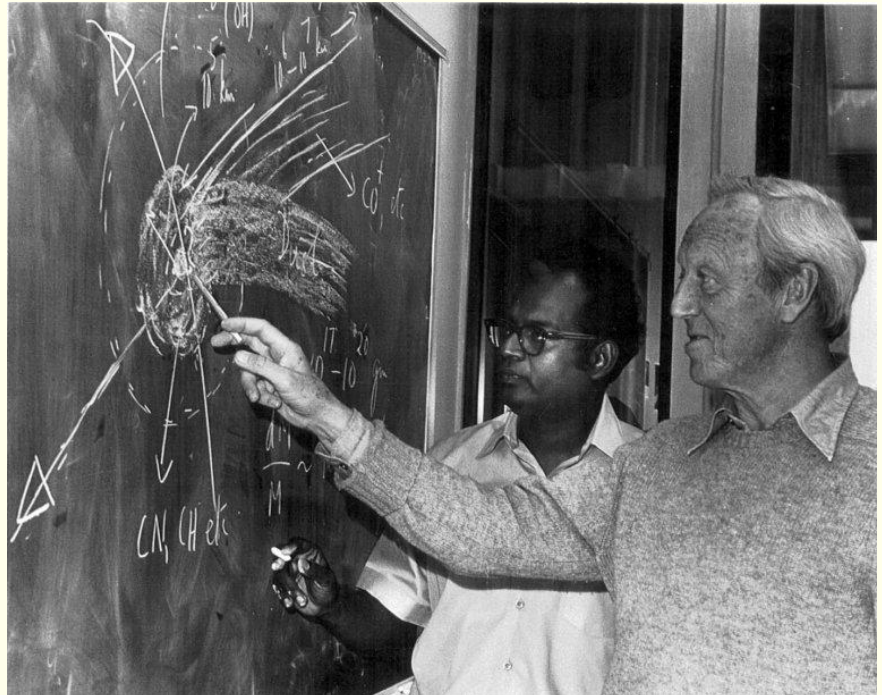
Intergalactic plasma

- Mostly made up of “bridges” between galaxies ($\sim 10^6$ l.y.) (Radius of Milky Way is $\sim 10^4$ l.y.)
- Detected by radio telescope measurements of synchrotron radiation from energetic electrons.
- Typical densities are 10^{-4} cm $^{-3}$
- Typical magnetic field: $B \sim 10^{-2}$ nT

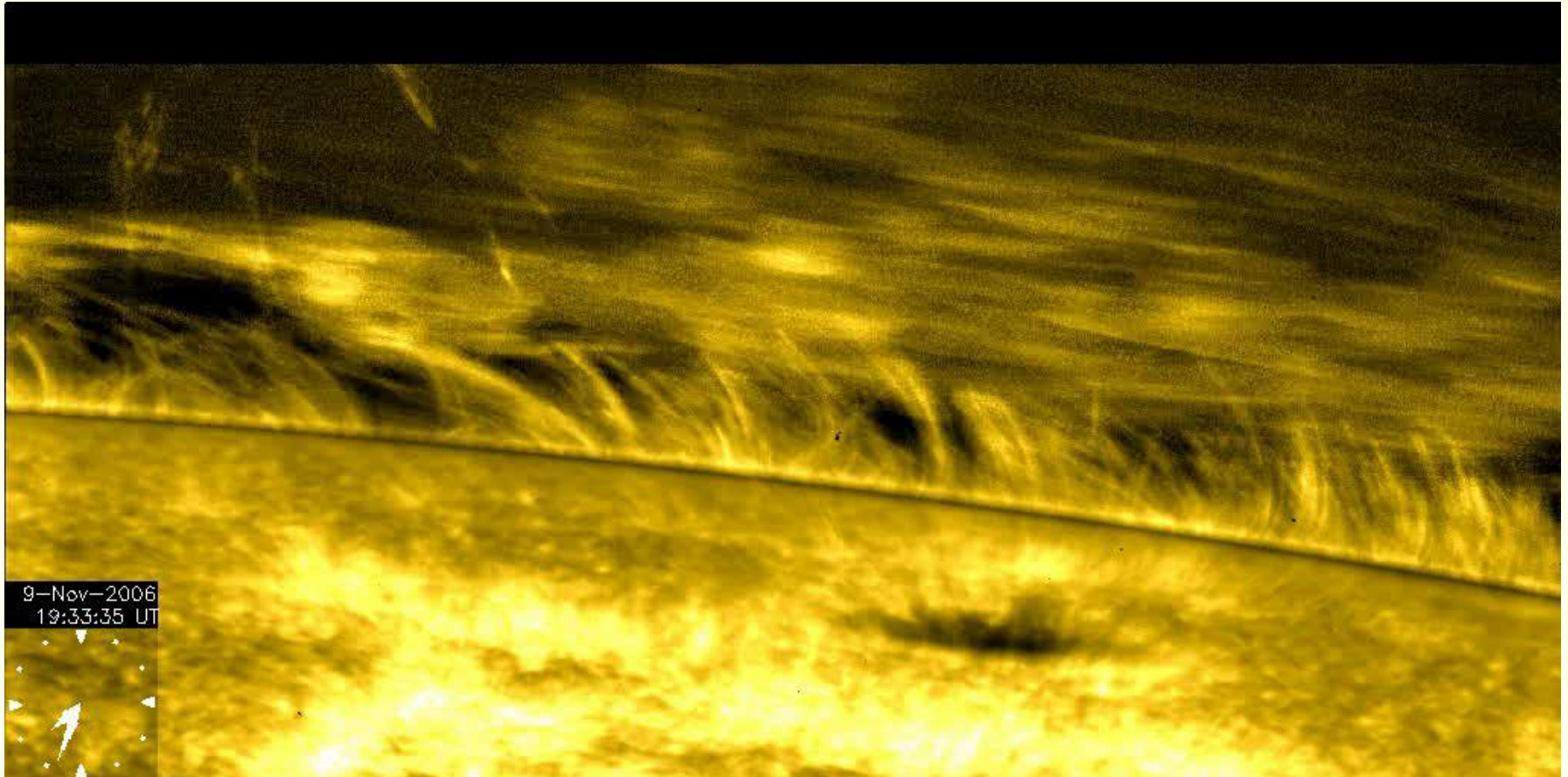
Alfvén waves

- Hannes Alfvén (1908-1995), professor at KTH
- Alfvén received the Nobel prize in 1970

'for fundamental work and discoveries in magneto-hydrodynamics with fruitful applications in different parts of plasma physics'



Alfvén waves



Solar corona

Alfvén waves

$$\frac{\partial \mathbf{B}}{\partial t} = -\nabla \times \mathbf{E} \quad (1)$$

$$\mathbf{j} = \sigma \mathbf{E}' = \sigma (\mathbf{E} + \mathbf{v} \times \mathbf{B}) \Rightarrow$$

$$\frac{\mathbf{j}}{\sigma} = (\mathbf{E} + \mathbf{v} \times \mathbf{B}) \Rightarrow$$

$$\mathbf{E} = -\mathbf{v} \times \mathbf{B} \quad (2)$$

$$\rho \left\{ \frac{\partial \mathbf{v}}{\partial t} + (\mathbf{v} \cdot \nabla) \mathbf{v} \right\} = -\cancel{\nabla p} + \mathbf{j} \times \mathbf{B} \quad (3)$$

$$\mu_0 \mathbf{j} = \nabla \times \mathbf{B} \quad (4)$$

$$\nabla \cdot \mathbf{v} = 0 \quad (5)$$

$$(1) + (2) \Rightarrow \frac{\partial \mathbf{B}}{\partial t} = \nabla \times (\mathbf{v} \times \mathbf{B}) \quad (6)$$

$$(3) + (4) \Rightarrow$$

$$\rho \left\{ \frac{\partial \mathbf{v}}{\partial t} + (\mathbf{v} \cdot \nabla) \mathbf{v} \right\} = \frac{1}{\mu_0} (\nabla \times \mathbf{B}) \times \mathbf{B} \quad (7)$$

Alfvén waves

Linearize

$$\mathbf{B} = \mathbf{B}_0 + \mathbf{B}_1$$

$$\mathbf{v} = \cancel{\mathbf{v}_0} + \mathbf{v}_1 = \mathbf{v}_1$$

$$(6) + (7) \Rightarrow$$

$$\frac{\partial \mathbf{B}_1}{\partial t} = \nabla \times (\mathbf{v}_1 \times \mathbf{B}_0) \quad (8)$$

$$\rho \frac{\partial \mathbf{v}_1}{\partial t} = \frac{1}{\mu_0} (\nabla \times \mathbf{B}_1) \times \mathbf{B}_0 \quad (9)$$

$$(8) + (9) \Rightarrow$$

$$\frac{\partial \mathbf{B}_1}{\partial t} = (\mathbf{B}_0 \cdot \nabla) \mathbf{v}_1 \quad (8')$$

$$\rho \frac{\partial \mathbf{v}_1}{\partial t} = \frac{1}{\mu_0} \left\{ -\nabla (\mathbf{B}_1 \cdot \mathbf{B}_0) + (\mathbf{B}_0 \cdot \nabla) \mathbf{B}_1 \right\} \quad (9')$$

Let $\mathbf{B}_0 = B_0 \hat{\mathbf{z}}$ and study waves along $\hat{\mathbf{z}}$

Alfvén waves

(8') \Rightarrow

$$\frac{\partial \mathbf{B}_1}{\partial t} = (B_0 \hat{\mathbf{z}} \cdot \nabla) \mathbf{v}_1 = B_0 \frac{\partial \mathbf{v}_1}{\partial z}$$

(9') \Rightarrow

$$\rho \frac{\partial \mathbf{v}_1}{\partial t} \frac{1}{\mu_0} \left\{ -\nabla (B_0 \hat{\mathbf{z}} \cdot \mathbf{B}_1) + B_0 \frac{\partial \mathbf{B}_1}{\partial z} \right\}$$

Thus

$$\begin{cases} \frac{\partial \mathbf{B}_1}{\partial t} = B_0 \frac{\partial \mathbf{v}_1}{\partial z} \\ \rho \frac{\partial \mathbf{v}_1}{\partial t} = \frac{1}{\mu_0} B_0 \frac{\partial \mathbf{B}_1}{\partial z} \end{cases}$$

\Rightarrow

$$\frac{\partial^2 \mathbf{B}_1}{\partial t^2} = \frac{B_0^2}{\mu_0 \rho} \frac{\partial^2 \mathbf{B}_1}{\partial z^2}$$

$$v = v_A = \frac{B_0}{\sqrt{\mu_0 \rho}}$$

Alfvén waves

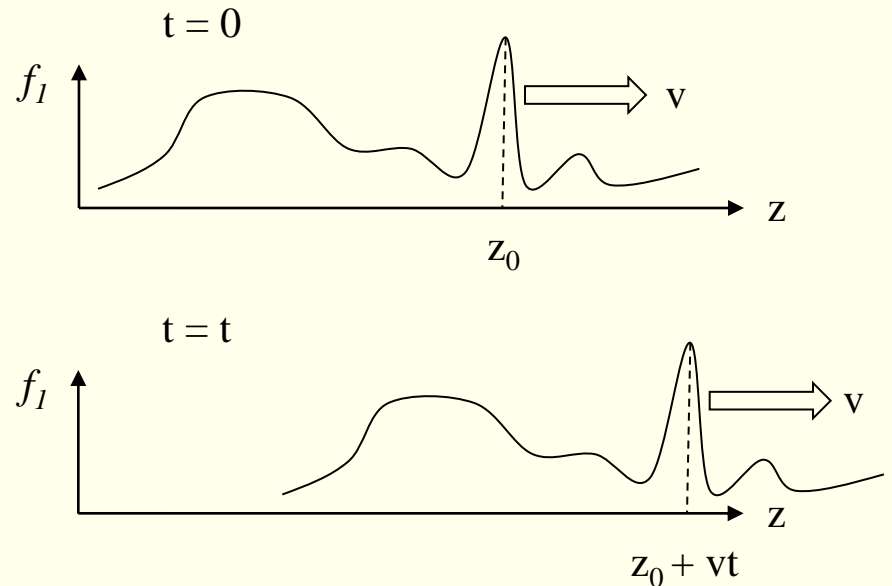
The wave equation

$$\frac{\partial^2 \mathbf{B}_1}{\partial t^2} = v^2 \frac{\partial^2 \mathbf{B}_1}{\partial z^2}$$

$$v = v_A = \frac{B_0}{\sqrt{\mu_0 \rho}}$$

has the general solution

$$\mathbf{B}_1 = \mathbf{f}_1(z - vt) + \mathbf{f}_2(z + vt)$$



In particular harmonic waves are solutions

$$\mathbf{B}_1 = \tilde{\mathbf{B}}_1 e^{i(kz - \omega t)} = \tilde{\mathbf{B}}_1 e^{ik(z - \frac{\omega}{k}t)} = \tilde{\mathbf{B}}_1 e^{ik(z - vt)}$$

Alfvén waves, polarization

$$\rho \frac{\partial \mathbf{v}_1}{\partial t} = \frac{1}{\mu_0} B_0 \frac{\partial \mathbf{B}_1}{\partial z}$$

Assuming harmonic waves, e.g:

$$\mathbf{B}_1 = \tilde{\mathbf{B}}_1 e^{i(k_z z - \omega t)}$$

$$-i\omega\rho\mathbf{v}_1 = \frac{ik_z}{\mu_0} B_0 \mathbf{B}_1 \quad \Rightarrow$$

$$-\frac{\omega}{k_z} \frac{\mu_0 \rho}{B_0} \mathbf{v}_1 = \mathbf{B}_1$$

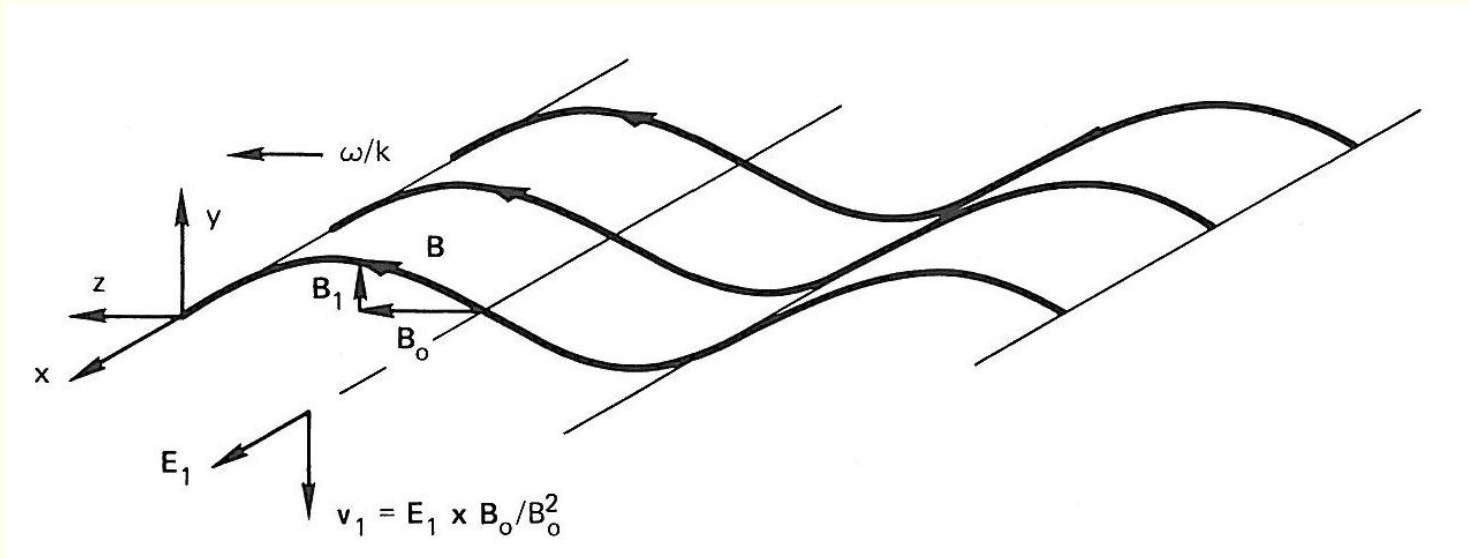
$$\frac{\partial \mathbf{B}}{\partial t} = -\nabla \times \mathbf{E} \quad \Rightarrow$$

$$-i\omega \mathbf{B}_1 = -ik_z \hat{\mathbf{z}} \times \mathbf{E}_1 \quad \Rightarrow$$

$$\omega B_{1y} = k_z E_{1x} \quad \Rightarrow$$

$$\frac{E_{1x}}{B_{1y}} = \frac{\omega}{k_z} = v_g = v_A$$

Alfvén waves, polarization



$$-\frac{\omega}{k_z} \frac{\mu_0 \rho}{B_0} \mathbf{v}_1 = \mathbf{B}_1$$

$$\frac{E_{1x}}{B_{1y}} = \frac{\omega}{k_z} = v_g = v_A$$

Alfvén waves

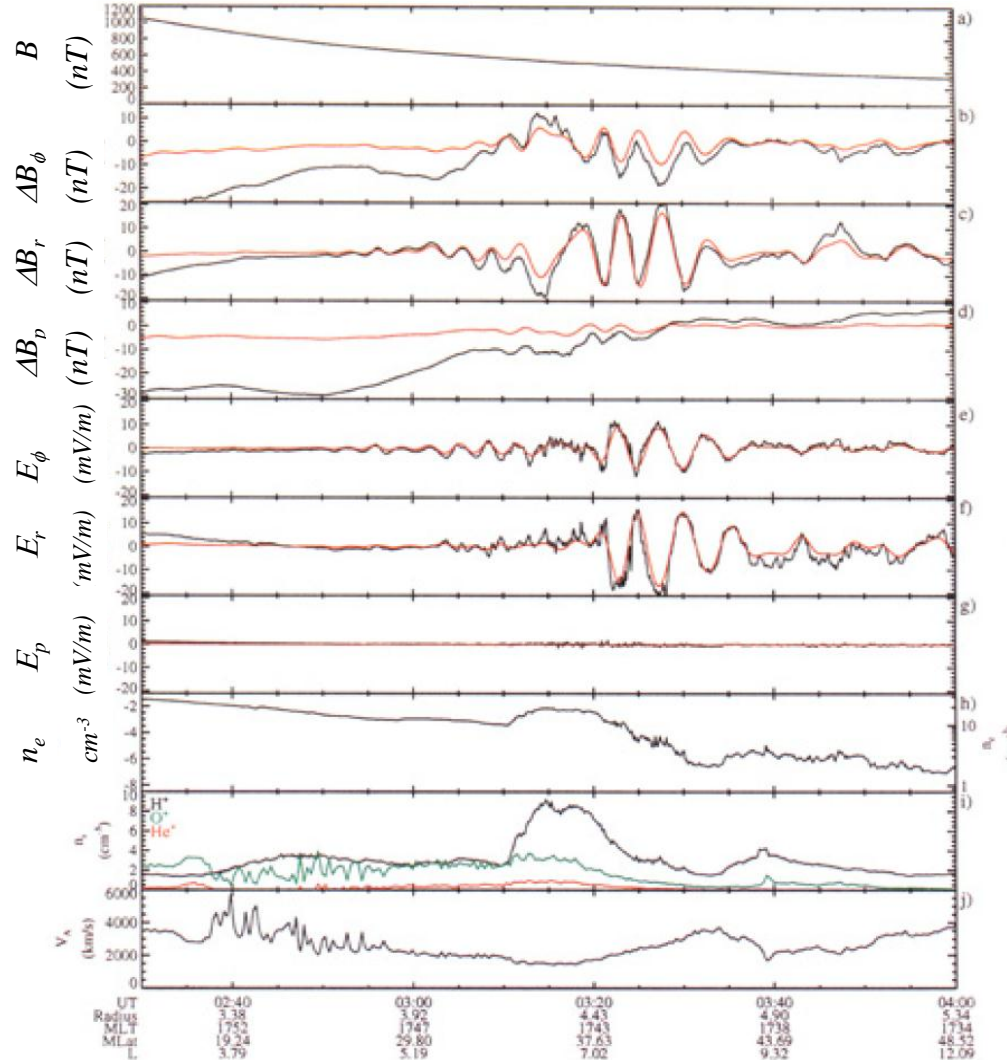
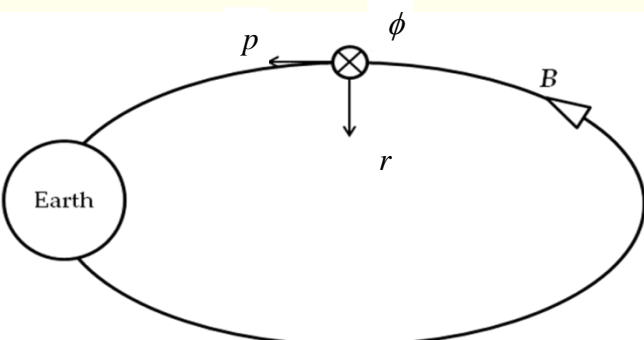


Plate 4. Measurements from Polar on January 11, 1997. (Plate 4a) Magnitude of the magnetic field. (Plates 4b-4d) Components of the deviation of the magnetic field from a model field in field-aligned coordinates (parallel to the average field, p ; perpendicular to p and generally along radius vector from Earth's center, r ; perpendicular to p and generally in the eastward azimuthal direction, ϕ). The red traces have been treated with a band-pass filter. (Plates 4e-4g) Same as Plates 4b-4d for the electric field. (Plate 4h) Spacecraft floating potential. An approximate density scale based on the work of Laakso and Pedersen [1998] has been added. (Plate 4i) Partial ion densities for H^+ (black), O^+ (green), and He^+ (red). (Plate 4j) Upper limit of the Alfvén speed based on the magnetic field in Plate 4a and the partial ion densities in Plate 4i.

Clemmons et al., 1999

What is the Alfvén velocity?

Blue

$$v_A \approx 200\,000 \text{ km/s}$$

Red

$$v_A \approx 20\,000 \text{ km/s}$$

Yellow

$$v_A \approx 2\,000 \text{ km/s}$$

Green

$$v_A \approx 20 \text{ km/s}$$

$$\frac{E_{1x}}{B_{1y}} = \frac{\omega}{k_z} = v_g = v_A$$

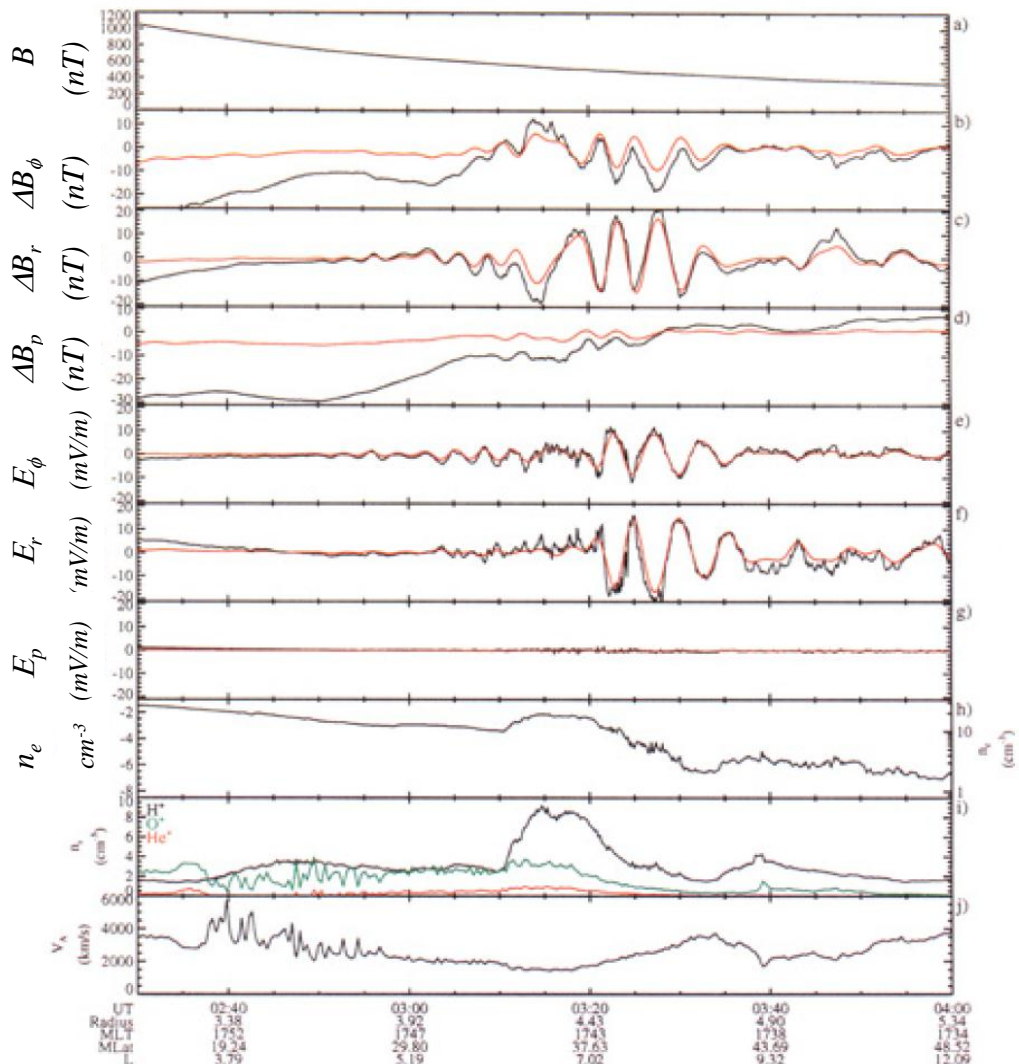


Plate 4. Measurements from Polar on January 11, 1997. (Plate 4a) Magnitude of the magnetic field. (Plates 4b-4d) Components of the deviation of the magnetic field from a model field in field-aligned coordinates (parallel to the average field, p ; perpendicular to p and generally along radius vector from Earth's center, r ; perpendicular to p and generally in the eastward azimuthal direction, ϕ). The red traces have been treated with a band-pass filter. (Plates 4e-4g) Same as Plates 4b-4d for the electric field. (Plate 4h) Spacecraft floating potential. An approximate density scale based on the work of Laakso and Pedersen [1998] has been added. (Plate 4i) Partial ion densities for H^+ (black), O^+ (green), and He^+ (red). (Plate 4j) Upper limit of the Alfvén speed based on the magnetic field in Plate 4a and the partial ion densities in Plate 4i.

What is the Alfvén velocity?

$$v_A = \frac{E_r}{B_\phi} \text{ ms}^{-1} = \frac{35 \cdot 10^{-3}}{20 \cdot 10^{-9}} \text{ ms}^{-1} = \\ = 1750 \text{ km s}^{-1}$$

Yellow

$$v_A \approx 2000 \text{ km/s}$$

$$v_A = \frac{B_0}{\sqrt{\mu_0 \rho}}$$

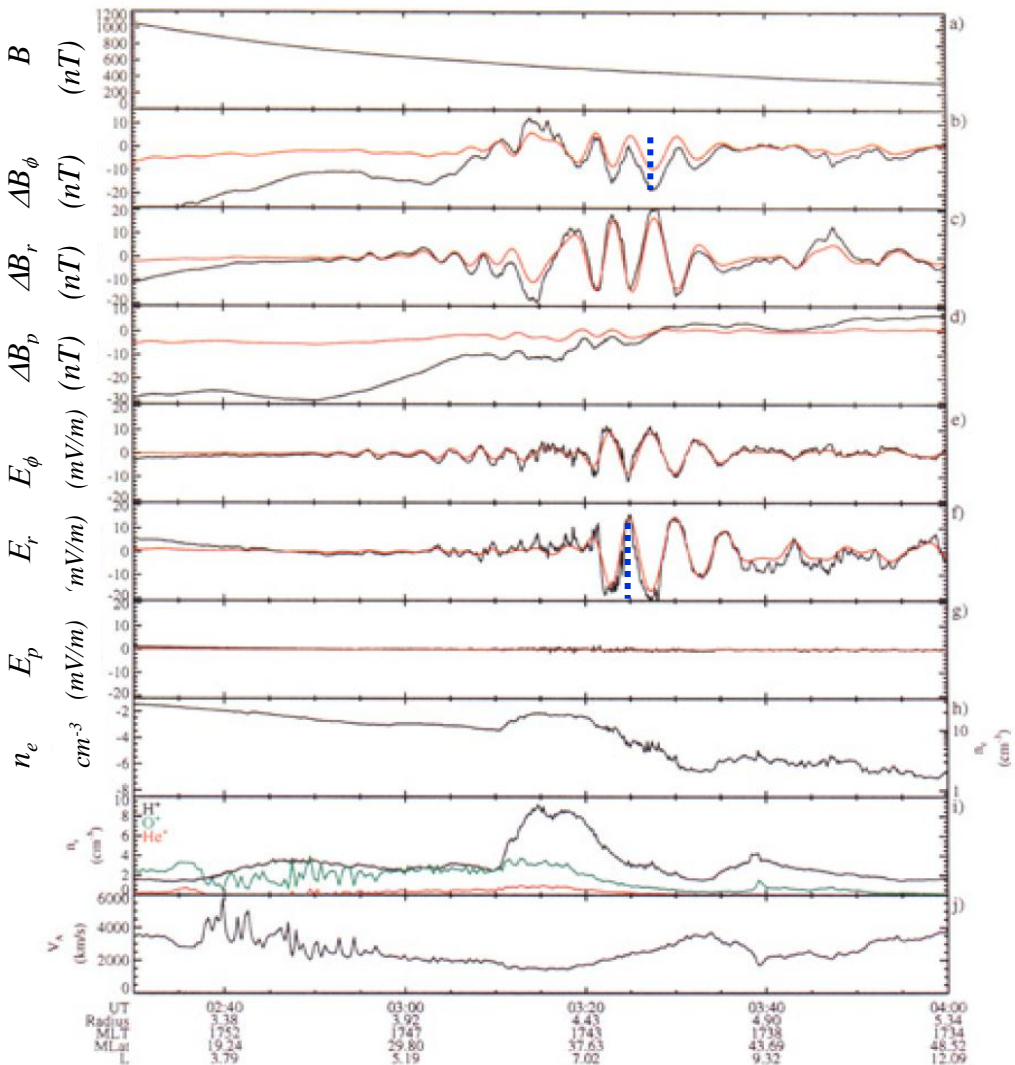
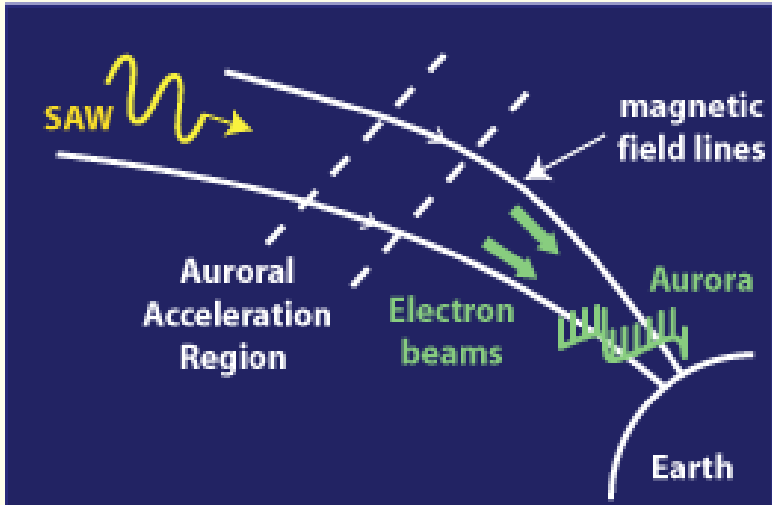
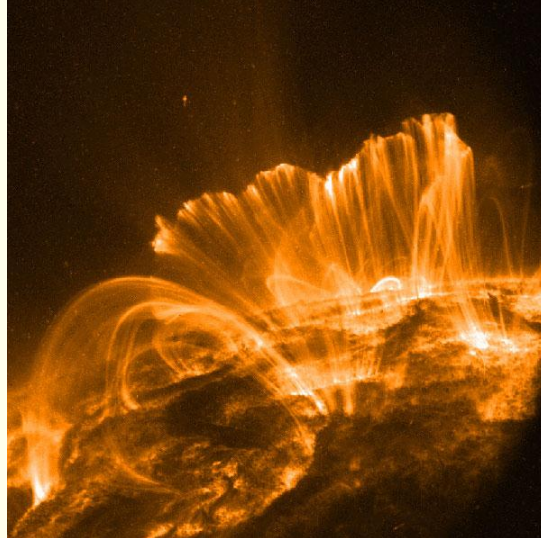


Plate 4. Measurements from Polar on January 11, 1997. (Plate 4a) Magnitude of the magnetic field. (Plates 4b-4d) Components of the deviation of the magnetic field from a model field in field-aligned coordinates (parallel to the average field, p ; perpendicular to p and generally along radius vector from Earth's center, r ; perpendicular to p and generally in the eastward azimuthal direction, ϕ). The red traces have been treated with a band-pass filter. (Plates 4e-4g) Same as Plates 4b-4d for the electric field. (Plate 4h) Spacecraft floating potential. An approximate density scale based on the work of Laakso and Pedersen [1998] has been added. (Plate 4i) Partial ion densities for H^+ (black), O^+ (green), and He^+ (red). (Plate 4j) Upper limit of the Alfvén speed based on the magnetic field in Plate 4a and the partial ion densities in Plate 4i.

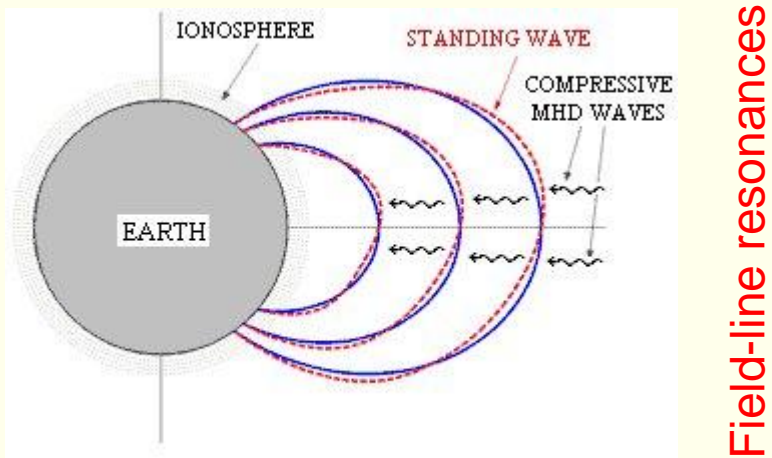
Alfvén waves



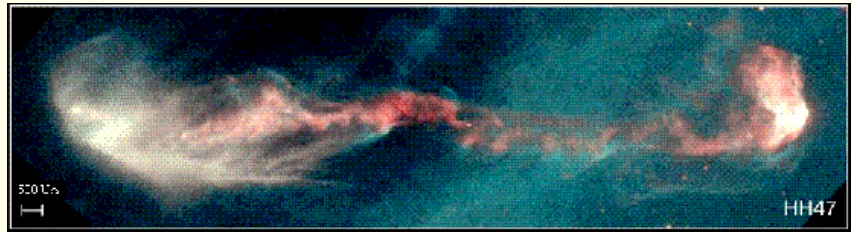
Auroral acceleration



Alfvén waves heating the solar corona?



Field-line resonances



Alfvén waves playing a role in dynamics of star formation in giant molecular clouds?